Zoosyst. Evol. 101 (4) 2025, 1621–1638 | DOI 10.3897/zse.101.156697

Taxonomic and distributional revision of *Pareas boulengeri* (Reptilia, Squamata, Pareidae), including two new species from eastern and central China

Cai-wen Zhang[1], Shi-hang Xu[1], Tao Luo[2], Chong Liu[1], Lei Yu[1], Jiang Zhou[3], Tao Pan[4], Bao-wei Zhang[1]

1 *School of Life Sciences, Anhui University, Hefei 230601, Anhui, China*
2 *School of Life Sciences, Yunnan University, Kunming, Yunnan 650091, China*
3 *School of Karst Science, Guizhou Normal University, Guiyang 550025, Guizhou, China*
4 *College of Life Sciences, Anhui Normal University, Wuhu 241000, Anhui, China*

https://zoobank.org/468C419C-151E-4AE4-AC9E-25FE3992945E

Corresponding authors: Bao-wei Zhang (zhangbw@ahu.edu.cn); Tao Pan (pantao@ahnu.edu.cn)

Academic editor: Justin Bernstein ♦ **Received** 23 April 2025 ♦ **Accepted** 1 July 2025 ♦ **Published** 2 September 2025

Abstract

The Boulenger's slug snake (*Pareas boulengeri* Angel, 1920) has previously been documented as relatively widely distributed across the eastern, southern, and southwestern regions of China. In the present study, integrated morphological comparisons and molecular phylogenetic analyses were undertaken to reevaluate the taxonomic status of *P. boulengeri* and to describe two new species: *Pareas dabieshanensis* **sp. nov.** and *Pareas orientalis* **sp. nov.** Phylogenetic reconstruction based on CYTB gene sequences indicated that populations previously identified as *P. boulengeri* comprise three distinct lineages: true *P. boulengeri*, *P. dabieshanensis* **sp. nov.**, and *P. orientalis* **sp. nov.** The two new species exhibit significant genetic divergence from their congeners, with uncorrected pairwise distances of 4.1–4.5%, consistent with interspecific divergence within the genus. Morphologically, *P. dabieshanensis* **sp. nov.** is distinguished by the presence of two subocular scales, the absence of preocular scales, and higher ventral (184–187) and subcaudal (68–74) counts. *P. orientalis* **sp. nov.** is characterized by a single preocular scale and fused subocular and postocular scales. The revised distributions restrict *P. boulengeri* to southwestern China, while the new species are confined to the Dabie Mountains (Anhui, Hubei, Henan) and eastern China (southern Anhui, Jiangsu, Jiangxi, Zhejiang), respectively. The non-overlapping ranges of *P. dabieshanensis* **sp. nov.** and *P. orientalis* **sp. nov.**, bisected by the Yangtze River, suggest that this major hydrological system acted as a biogeographic barrier driving speciation. This study expands the genus *Pareas* to 33 recognized species (27 in China) and underscores the prevalence of cryptic diversity within morphologically conserved lineages.

Key Words

Cryptic species, geographic isolation, molecular phylogeny, morphology, speciation, Yangtze River

Introduction

Species of *Pareas* Wagler, 1830 (Squamata, Pareidae) are snail-eating or slug-eating, small, slender, arboreal nocturnal snakes. They possess a blunt snout, lack a mental groove, and have no teeth on the anterior maxilla (Hoso et al. 2007; Wallach et al. 2014; You et al. 2015; Poyarkov et al. 2022; Liu et al. 2023a). Their unique behavioral adaptation provides a considerable advantage within their ecological niche, allowing them to inhabit a vast region, including northeastern India, Myanmar, southern and eastern China, Indochina, and Sundaland. This broad distribution has ultimately led to the evolution of a diverse variety of species (You et al. 2015; Wang et al. 2020; Le et al. 2021; Liu and Rao 2021; Vogel et al. 2021; Poyarkov et al. 2022; Gong et al. 2023; Liu et al. 2023a, 2023b, 2024; Uetz et al. 2025). However, recent studies have suggested that the species diversity of *Pareas* has been severely underestimated, with 13 new species described and 8 resurrected since 2015 (Uetz et al. 2024). Thus, the genus *Pareas* now comprises

Copyright *Zhang, C.-w. et al.* This is an open access article distributed under the terms of the Creative Commons Attribution License (CC BY 4.0), which permits unrestricted use, distribution, and reproduction in any medium, provided the original author and source are credited.

31 recognized species (Uetz et al. 2024), 22 of which are distributed in China (Liu et al. 2024; Uetz et al. 2025).

Among *Pareas* congeners, *P. boulengeri* (Angel, 1920) has a relatively wide distribution. This species was originally described based on a specimen from Guizhou Province in southwest China and named after George Albert Boulenger, a herpetologist at the British Museum of Natural History, London. Subsequently, *P. boulengeri* has been reported in multiple localities across eastern, southern, and southeastern China (Chen 1991; Zhao et al. 1998; Chen et al. 2006; Guo and Deng 2006; Zhao 2006). Notably, cryptic species have recently been identified within certain widespread *Pareas* species (Wang et al. 2020; Wu et al. 2023). Prior research has indicated genetic differentiation among *P. boulengeri* populations in Huangshan (Anhui) and the Dabie Mountains and in Henan Province (Wu et al. 2023). However, the phylogenetic relationships and taxonomic status of populations recorded as *P. boulengeri* in eastern and southwestern China remain undefined.

This study presents a detailed morphological examination and phylogenetic analysis of populations formerly identified as *Pareas boulengeri*. In addition, the species boundaries and distribution of *P. boulengeri* are redefined, and two new species from the Dabie Mountains and eastern China are described.

Materials and methods

Sampling

This study was approved by the Institutional Animal Care and Use Committee of the School of Life Sciences at Anhui University (project number IACUC(AHU)-2022-050). We collected twenty-one specimens (13 adult females and 8 adult males) previously classified as *Pareas boulengeri*: 12 (females: 3, males: 9) from Anhui and Zhejiang provinces and 9 (females: 5, males: 4) from Guizhou Province, China (Fig. 1). After photographing the individuals, they were euthanized using isoflurane, fixed in 10% formaldehyde for two days, and subsequently washed and preserved in 75% ethanol. Liver tissue samples were collected from all specimens and preserved in 95% ethanol before fixation. The new vouchered specimens were deposited at the Anhui University Biology Museum (AHUBM).

In addition, 18 *P. boulengeri* samples from various sources (Table 1), along with their respective sampling localities, were obtained from the National Center for Biotechnology Information (NCBI). Distribution records for *P. boulengeri* were also downloaded from the Global Biodiversity Information Facility (GBIF) to update the species' distribution range (Fig. 1).

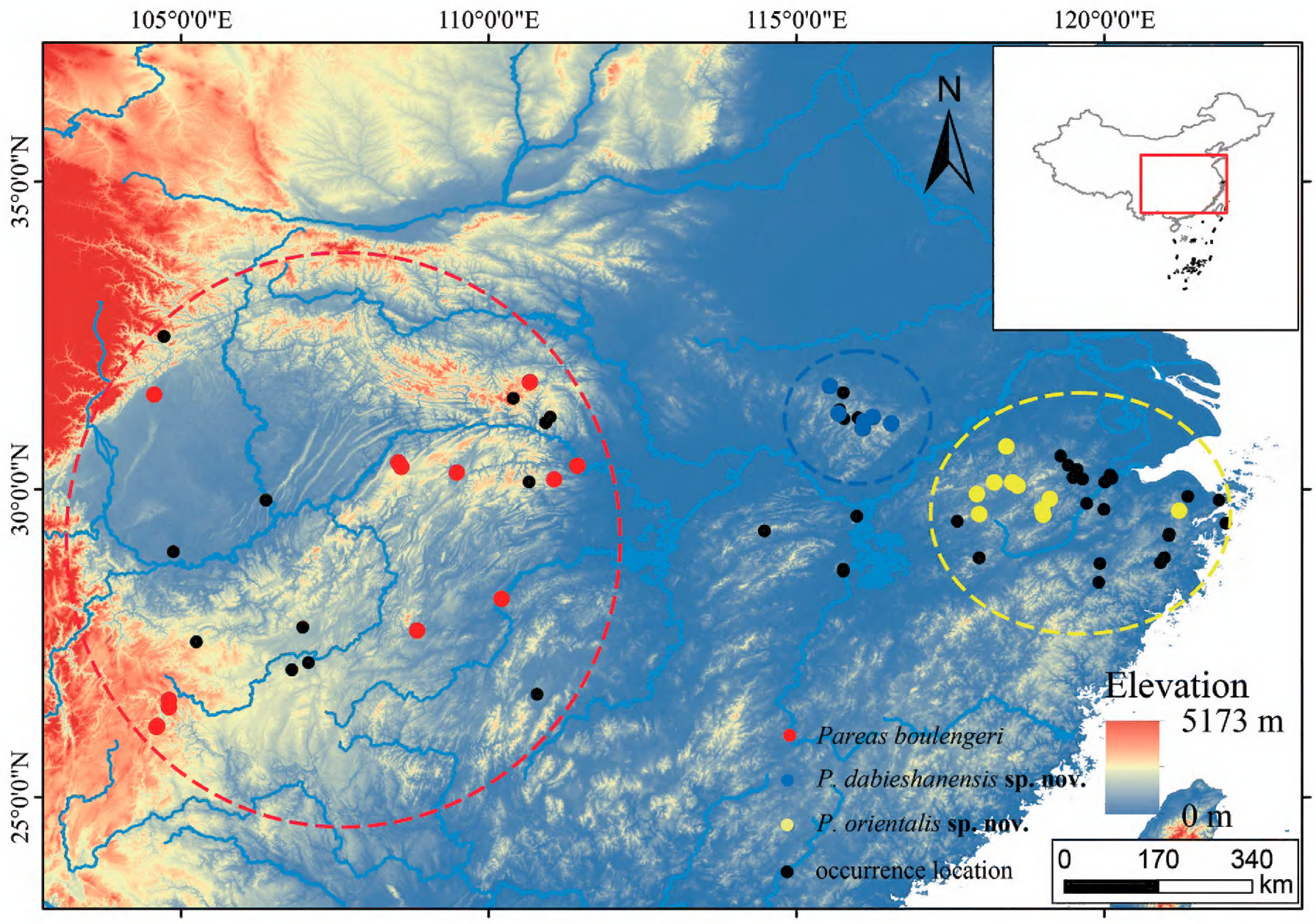

Figure 1. Data locations pertinent to this research. The black dots indicate current distribution points of *Pareas boulengeri*, as documented in GBIF. The red, blue, and yellow circles denote the sampling sites for *P. boulengeri*, *P. dabieshanensis*, and *P. orientalis*, respectively. This map includes both actual sampling sites and approximate locations associated with sequence data obtained from NCBI. The dotted circles in red, blue, and yellow represent the potential distribution ranges of the three species under investigation.

Table 1. Samples used in the molecular analyses, including GenBank numbers, voucher IDs, and localities.

ID	Species	Locality	Voucher ID	GenBank no.	Source
1	*P. abros*	Song Thanh, Quang Nam, Vietnam	ZMMU R-16393	MZ712235	Poyarkov et al. 2022
2	*P. andersonii*	Mt. Natmataung, Chin, Myanmar	CAS 235359	MT968772	Vogel et al. 2020
3	*P. atayal*	N. Cross Is. Hw., Taiwan, China	NMNS 05594	KJ642122	You et al. 2015
4	*P. baiseensis*	Baise, Guangxi, China	ANU000220008	OQ054329	Gong et al. 2023
5	*P. berdmorei*	Kin Pon Chaung, Mon, Myanmar	CAS 240362	MZ712219	Poyarkov et al. 2022
6	*P. boulengeri*	Jiangkou, Guizhou, China	GP 2923	MK135090	Wang et al. 2020
7	*P. boulengeri*	Anxian, Sichuan, China	GP 207	MK135091	Wang et al. 2020
8	*P. boulengeri*	Wufeng, Hubei, China	YBU 13323A	MK135092	Wang et al. 2020
9	*P. boulengeri*	Yidu, Hubei, China	GP 4716	MK135093	Wang et al. 2020
10	*P. boulengeri*	Fenghua, Zhejiang, China	SYSr001769	MK201584	Li et al. 2020
11	*P. boulengeri*	Yixian, Anhui, China	GP 3428	MK135094	Wang et al. 2020
12	*P. boulengeri*	Chunan, Zhejiang, China	YBU 17155	MK135095	Wang et al. 2020
13	*P. boulengeri*	Chunan, Zhejiang, China	YBU 17245	MK135096	Wang et al. 2020
14	*P. boulengeri*	Mianyang, Sichuan, China	HS09001	MK201240	Li et al. 2020
15	*P. boulengeri*	Huangshan, Anhui, China	HS14024	MK201241	Li et al. 2020
16	*P. boulengeri*	Enshi, Hubei, China	KIZ 09965	JF827678	Guo et al. 2011
17	*P. boulengeri*	jiannan, Hubei, China	KIZ 09966	JF827679	Guo et al. 2011
18	*P. boulengeri*	jianzhuxi, Hubei, China	KIZ 09967	JF827680	Guo et al. 2011
19	*P. boulengeri*	Luxi,Hunan, China	KIZ 09968	JF827681	Guo et al. 2011
20	*P. boulengeri*	Shennongjia, Hubei, China	KIZ 09969	JF827682	Guo et al. 2011
21	*P. boulengeri*	Luxi,Hunan, China	KIZ 09970	JF827683	Guo et al. 2011
22	*P. boulengeri*	Shennongjia, Hubei, China	KIZ 09971	JF827684	Guo et al. 2011
23	*P. boulengeri*	Qimen, Anhui, China	HSR18074	MN866896	Huang et al. 2020
24	*P. boulengeri*	Huangping, Guizhou, China	GZNU2018051502	PV804873	This study
25	*P. boulengeri*	Huangping, Guizhou, China	GZNU2018051503	PV804874	This study
26	*P. boulengeri*	Huangping, Guizhou, China	GZNU20180515017	PV804875	This study
27	*P. boulengeri*	Liupangshui, Guizhou, China	LPSSY2024070903	PV804876	This study
28	*P. boulengeri*	Liupangshui, Guizhou, China	LPSSY2022070601	PV804877	This study
29	*P. dabieshanensis* sp. nov.	Jinzhai, Anhui,China	AHU2024042601	PV804864	This study
30	*P. dabieshanensis* sp. nov.	Yuexi, Anhui,China	AHU2014100801	PV804866	This study
31	*P. dabieshanensis* sp. nov.	Huoshan, Anhui, China	AHU2021050201	PV804865	This study
32	*P. dabieshanensis* sp. nov.	Huoshan, Anhui, China	AHU2024042601	PV804867	This study
33	*P. orientalis* sp. nov.	Chunan, Zhejiang, China	AHU2021101501	PV804869	This study
34	*P. orientalis* sp. nov.	Jing, Anhui, China	AHU2019061201	PV804868	This study
35	*P. orientalis* sp. nov.	Xiuning, Anhui, China	AHU2024110501	PV804870	This study
36	*P. orientalis* sp. nov.	Huangshan, Anhui, China	AHU2024072201	PV804871	This study
37	*P. orientalis* sp. nov.	Xiuning, Anhui, China	AHU2024051502	PV804872	This study
38	*P. carinatus*	Sungai Sedim, Kedah, Malaysia	LSUHC10604	KC916748	Loredo et al. 2013
39	*P. chinensis*	Hongya, Sichuan, China	GP 2383	MK135089	Wang et al. 2020
40	*P. dulongjiangensis*	Gongshan, Yunnan, China	KIZ R201607	OQ718498	Liu et al. 2023b
41	*P. formosensis*	N. Cross Is. Hw., Taiwan, China	NMNS 05632	KJ642130	You et al. 2015
42	*P. geminatus*	Jiangcheng, Yunnan, China	CIB 118021	MW287068	Ding et al. 2020
43	*P. guanyinshanensis*	Yuanyang, Yunnan, China	KIZ 2023038	PP215390	Liu et al. 2023a
44	*P. hamptoni*	Kachin, Myanmar,	YPX 18219	MK135077	Wang et al. 2020
45	*P. iwasakii*	Ishigaki Is., S. Ryukyu, Japan	I03-ISG1	KJ642158	You et al. 2015
46	*P. kaduri*	Lohit, Arunachal, India	BNHS 3574	MT188734	Bhosale et al. 2020
47	*P. komaii*	Lijia, Taitung, Taiwan, China	HC 000669	JF827687	Guo et al. 2011
48	*P. kuznetsovorum*	Song Hinh, Phu Yen, Vietnam	ZMMU R-16802	MZ712232	Poyarkov et al. 2022
49	*P. macularius*	Bago, Myanmar	CAS 206620	AF471082	Guo et al. 2011
50	*P. margaritophorus*	Cangwu, Guangxi, China	YBU 16061	MK135097	Wang et al. 2020
51	*P. modestus*	Tanhril, Aizawl, Mizoram, India	MZMU 1293	MT968773	Vogel et al. 2020
52	*P. monticola*	Medog, Tibet, China	GP 2027	MK135107	Wang et al. 2020
53	*P. niger*	Kunming, Yunnan, China	KIZ 059339	MW436706	Liu and Rao 2021
54	*P. nigriceps*	Mt. Gaoligong, Yunnan, China	SYSr001222	MK201455	Li et al. 2020
55	*P. nuchalis*	Belait, Brunei	FK 2626	MZ603794	Le et al. 2021
56	*P. stanleyi*	Guilin, Guangxi, China	HM 2007-S001	JN230704	Guo et al. 2011
57	*P. temporalis*	Da Huoai, Lam Dong, Vietnam	UNS 09992	MZ603793	Le et al. 2021
58	*P. tigerinus*	Menghai, Yunnan, China	KIZ 20210703	OP752143	Liu et al. 2023b
59	*P. victorianus*	Mt. Natmataung, Chin, Myanmar	CAS 235254	MW438300	Vogel et al. 2021
60	*P. vindumi*	Lukpwir, Kachin, Myanmar	CAS 248147	MT968776	Vogel et al. 2020
61	*P. xuelinensis*	Lancang, Yunnan, China	KIZ XL1	MW436709	Liu and Rao 2021
62	*P. yunnanensis*	Dali, Yunnan, China,	KIZ 2022033	OP752146	Liu et al. 2023a
63	*Aplopeltura boa*	Malaysia	LSUHC 7248	KC916746	Loredo et al. 2013

Molecular data and phylogenetic analyses

Purified DNA was extracted from liver tissue using a standard phenol/chloroform extraction method (Sambrook et al. 1989). Partial sequences of the mitochondrial cytochrome *b* gene (CYTB) were amplified and sequenced using the following primers: L14910 (5′-GACCTGTGATMTGAAAACCAYCGTTGT-3′) and H16064 (5′-CTTTGGTTTACAAGAACAATGCTTTA-3′) (Lawson et al. 2005). Polymerase chain reaction (PCR) was conducted in a 25-μL volume. Each reaction contained 100 ng of template DNA, 0.3 mM of each primer, and 10 μL of Premix Ex Taq™ (Takara). The PCR protocol included an initial denaturation at 94 °C for 3 min; followed by 35 cycles of denaturation at 94 °C for 30 s, annealing at 52 °C for 40 s, and extension at 72 °C for 90 s; and a final extension at 72 °C for 10 min. PCR products were purified using an EasyPure PCR Purification Kit, following the manufacturer's instructions (TransGene). Each fragment was sequenced bidirectionally using an ABI 3730 semi-automated sequencer (PE Applied Biosystems). Amplified products were submitted to General Biology (Anhui) Co., Ltd. (Chuzhou, China), and resulting sequences were deposited in GenBank (accession numbers provided in Table 1).

According to the species list on the Reptile Database (Uetz et al. 2025), gene sequences of all recognized *Pareas* species were downloaded from GenBank to enable comprehensive phylogenetic comparisons. Additionally, sequences for *Aplopeltura boa* were obtained from GenBank and used as the outgroup. A total of 105 sequences from 47 individuals representing 16 species were included (Table 1).

CYTB sequence alignment was performed using MAFFT 7.110 with the G-INS-i algorithm (Katoh et al. 2005; Katoh and Standley 2013). The resulting alignments were trimmed with BioEdit 7.0.5.3 to remove low-quality bases at both ends (Hall 1999), and the final dataset was manually merged. jModelTest was used to select the best-fitting evolutionary model based on the corrected Akaike Information Criterion (AIC) (Guindon and Gascuel 2003; Posada 2008; Akaike 1974). The best-fitting model was selected by comparing the log-likelihood, AIC, and BIC values across multiple models, choosing the one with the lowest AIC or BIC (Akaike 1974). Bayesian inference (BI) was performed using MrBayes 3.2.4 (Ronquist et al. 2012), and maximum likelihood (ML) analysis was conducted using RAxMLGUI 1.3 (Silvestro and Michalak 2012). For BI, two parallel runs of 10,000,000 generations were executed, with trees sampled every 1,000 generations. The first 25% of samples were discarded as burn-in, and the remaining trees were used to generate a 50% majority-rule consensus tree. Bayesian posterior probabilities (BPPs) were calculated. The potential scale reduction factor (PSRF) was < 0.005, and the error rate was < 0.01. Markov Chain Monte Carlo (MCMC) convergence was assessed using Tracer v1.5 (Rambaut et al. 2024), confirming that all effective sample sizes (ESSs) exceeded 200 and PSRFs were close to 1.0.

Morphological analyses

In accordance with previous studies (Dowling 1951; Zhao 2006; Vogel 2015), 22 commonly used morphological characteristics were assessed in adult slug-eating snake samples, comprising 6 mensural and 16 meristic traits, using established terminologies and methods. Body morphological measurements were typically recorded to the nearest 1 mm using a measuring tape, while others were recorded to the nearest 0.1 mm using an electronic slide caliper. The morphological measurements included snout–vent length (SVL), the distance from the tip of the snout to the posterior edge of the vent; tail length (TaL); total length (TL), the distance from the snout tip to the tail end; relative tail length (TaL/TL); head length (HL), the distance from the snout tip to the jaw angles; maximal head width (HW), the distance across the widest part of the head; and eye diameter (ED), the distance from the anterior corner to the posterior corner of the eye.

The meristic characteristics evaluated included the number of dorsal scale rows counted at one head length behind the head (ASR), midbody (MSR, specifically at SVL/2), and one head length before the vent (PSR); enlarged vertebral scale rows (VSE); keeled dorsal scale rows at midbody (KMD); ventral scales (VEN); subcaudal scales (SC); cloacal plates (CP); supralabials (SPL); infralabials (IFL); anterior temporals (At); posterior temporals (Pt); loreals (LOR); preoculars (Preoc); suboculars (SoO); and postoculars (PoO). The values for paired head characteristics were recorded on both sides of the head in a left/right order.

Comparative data for various species were obtained from pertinent publications, including those by Boulenger (1900, 1905, 1914), Ota et al. (1997), Zhao et al. (1998), Malkmus et al. (2002), Guo and Zhao (2004), Jiang (2004), Zhao (2006), Guo and Deng (2006), Stuebing et al. (2014), Vogel (2015), You et al. (2015), Bhosale et al. (2020), Ding et al. (2020), Suntrarachun et al. (2020), Vogel et al. (2020), Wang et al. (2020), Le et al. (2021), Liu and Rao (2021), Vogel et al. (2021), Poyarkov et al. (2022), Gong et al. (2023), Liu et al. (2023a, 2023b), Oskyrko et al. (2024), and Liu et al. (2024).

Teeth counts and dentition asymmetry

X-ray scanning was conducted using nano-computed tomography. Specimens were examined with a GE v|tome|x m dual-tube 300/180 kV system at the Institute of Vertebrate Paleontology and Paleoanthropology (IVPP), Chinese Academy of Sciences. Each specimen was scanned with an energy beam of 80 kV and a flux of 80 μA, employing a 360° rotation. The data were subsequently reconstructed into a 4096 × 4096 matrix comprising 1,536 slices. The final computed tomography (CT)–reconstructed skull images were exported, achieving a spatial resolution of approximately 6.1 μm. The skull images were derived from virtual three-dimensional models reconstructed

using Volume Graphics Studio 3.0. The quantities of maxillary teeth (MX), palatine teeth (PAL), pterygoid teeth (PT), and dentary teeth (DT) were enumerated.

Results

Phylogenetic analyses

The aligned dataset comprised genes from 62 individuals of the *Pareas* genus and one from the outgroup *Aplopeltura boa* (Table 1). The dataset for the CYTB regions included 63 collections representing 34 taxa, resulting in a concatenated alignment of 1,096 characters. GTR + I + G was identified as the best-fit evolutionary model. The maximum likelihood (ML) search was terminated after 200 bootstrap (BS) replicates. For the Bayesian inference (BI), all chains converged after 2 million generations, with an average standard deviation of split frequencies of 0.006923 and an average ESS of 1,450. The ML and BI algorithms produced similar topologies for the main lineages; therefore, only the topology generated by the ML algorithm is presented, with BS values and BPPs > 50% and 0.90, respectively, shown at the nodes (Fig. 2).

Three independent lineages were identified within the 32 specimens previously classified as *Pareas boulengeri*. The samples from western China, the Dabie Mountains, and eastern China formed distinct lineages, each exhibiting strong support and low intra-lineage divergence. The two unnamed lineages (Dabie Mountains group and eastern China group) were identified as sister taxa and were closely related to *P. boulengeri* (western China group).

Genetic distances based on the CYTB gene among *Pareas* species are presented in Suppl. material 1: table S1. The two putative new species from the Dabie Mountains and eastern China exhibited significant genetic divergence from other congeners. Compared to closely related recognized congeners, the minimum uncorrected genetic distance was 4.1% between the clades from the Dabie Mountains and eastern China. Additionally, the minimum uncorrected genetic distances between the unnamed species and *P. boulengeri* from western China were 4.3% (between *P. boulengeri* and the Dabie Mountains group) and 4.5% (between *P. boulengeri* and the eastern China group). These distances were comparable to the interspecific distances among other recognized congeners, such as 4.3% between *P. hamptoni* and *P. guanyinshanensis* and 4.1% between *P. yunnanensis* and *P. geminatus* (Suppl. material 1: table S1).

Taxonomic account

Combining molecular phylogenetic analysis and morphological comparisons indicated that specimens from the Dabie Mountains and eastern China (southern Anhui, Jiangxi, and Zhejiang), previously classified as *Pareas boulengeri*, are distinct from the type locality and significantly differ from other known species within the genus *Pareas*. Accordingly, comprehensive taxonomic accounts and updated diagnoses for *P. boulengeri* were prepared, and the two new species were characterized.

Pareas Boulengeri (Angel, 1920)

Amblycephalus Boulengeri (Angel, 1920).
Amblycephalus monticola boulengeri (Mell, 1931).
Pareas boulengeri (Hu et al. 1973; Zhao et al. 1998, Chen et al. 2006; Guo and Deng 2006; Zhao 2006; Wallach et al. 2014; Vogel 2015).
Pareas (*Eberhardtia*) *boulengeri* (Poyarkov et al. 2022).

Type locality. Région de Koeï Tchéou, Chine." [=Guizhou region, southeastern China, ca. 27°N, 107°E].

Syntypes. MNHN-RA 1912.0349 (470 mm specimen), MNHN-RA 1912.0350 (82 mm specimen), and MNHN-RA 1912.0351 (460 mm specimen) (Révérend Père avalerie).

Specimens examined. Nine specimens were assessed (3 females and 6 males); all were molecularly identified as the species *Pareas boulengeri*. Four of the specimens were obtained from Liupanshui Normal University in Shuicheng City, Guizhou Province, China, with the following identifiers: LPSSY2024070903 (male), LPASY2022070601 (male), LPSSY2021070801 (female), and LPSSY2024070902 (female). One specimen was collected from the Shuicheng District of Liupanshui City: LPSSC2024070502 (female). One specimen was obtained from Yushe National Forest Park in Shuicheng City, Liupanshui City: LPSYS2022062802 (female). The remaining three specimens were obtained from Huangping County, Qiandongnan Miao and Dong Autonomous Prefecture, Guizhou Province: GZNU20180515017 (female), GZNU2018052303 (male), and GZNU2018052302 (male).

Common name. The common English name is Boulenger's Slug Snake; the common Chinese name is 平鳞钝头蛇 (Píng Lín Dùn Tóu Shé).

Etymology. Revised diagnosis: *Pareas boulengeri* can be distinguished from its congeners by a combination of the following characteristics (Fig. 3): (1) medium body size (TL 308–566 mm, n = 5 females; 362–565 mm, n = 6 males); (2) gray–brown or tan body, with many dorsal scales and covered with dark brown spots; (3) length of suture between internasals is distinctly shorter than that between the prefrontals, with a prefrontal bordering orbit; (4) frontal is subhexagonal to diamond-shaped, with its lateral sides converging posteriorly; (5) anterior pair of chin shields is longer than broad, with the loreal bordering the orbit; (6) the prefrontal contacts the eye, and there is one subocular scale with no preocular scales; (7) 7–8 supralabials and 9 infralabial scales; (8) rows of 15-15-15 dorsal scales, mid-dorsal scales smooth, and the vertebral scale row is not enlarged; (9) 175–188 ventrals scales, 57–66 subcaudals scales, divided, with a single cloacal plate; (10) prefrontal and postfrontal bones exhibit contact, asymmetric teeth number in maxilla, palatine, pterygoid, and dentary bones (MX 4–5/5, PAL 3/3,

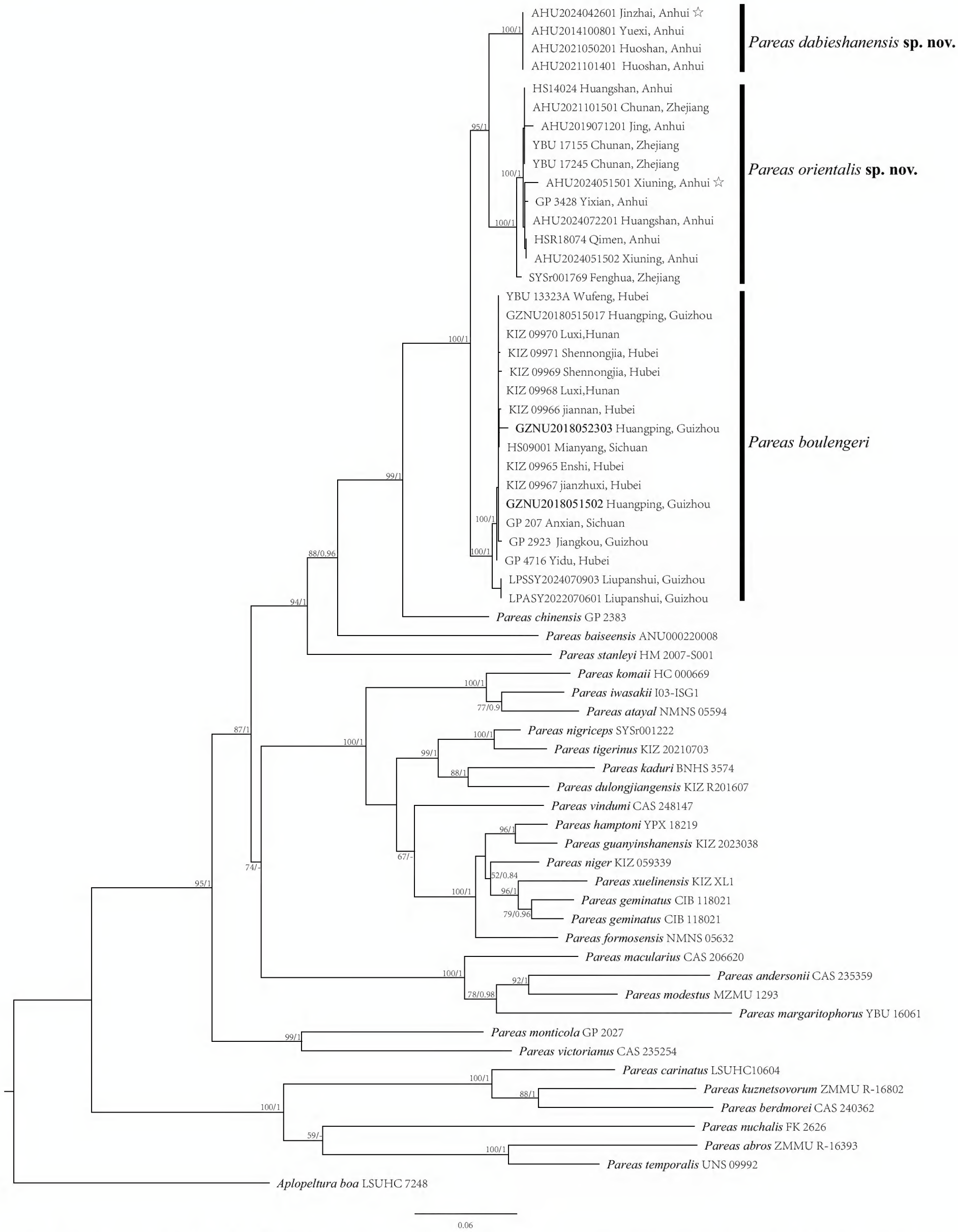

Figure 2. Maximum likelihood and Bayesian inference phylogenies based on mitochondrial CYTB genes. ML bootstrap support (BS)/Bayesian posterior probabilities (PP) are shown at nodes. Values are not displayed if BS < 50 or PP < 0.90. "white star" indicates holotype gene sequences.

PT9–13/9–11, DT 16–18/20–21); (11) dorsal surface of the head displays a dense configuration of black, coarse spots; two black longitudinal stripes extend posteriorly, located behind the parietal and supraocular scales, converging into a prominent black stripe in the neck region; a slender black horizontal line is present on the lateral aspect of the head, posterior to the eye and extending toward the corner of the mouth.

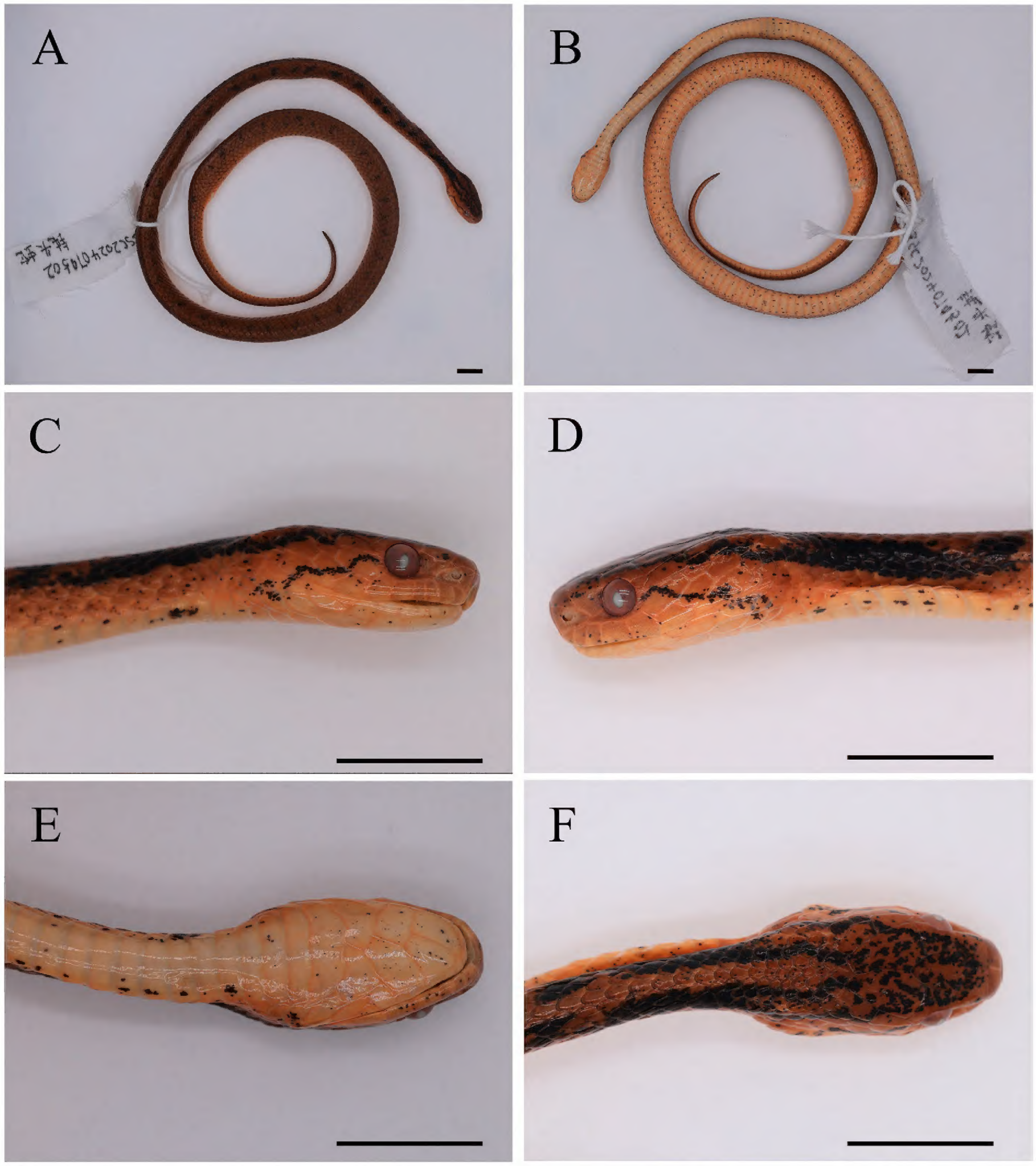

Figure 3. *Pareas boulengeri* in preservative (LPSSC2024070502). **A.** Dorsal view; **B.** Ventral view; **C.** Right lateral view of the head; **D.** Left lateral view of the head; **E.** Ventral view of the head; **F.** Dorsal view of the head. Scale bars: 10 mm.

Remarks. The type locality of *Pareas boulengeri* is in the "Région de Koeï Tchéou, Chine" [=Guizhou region, southeastern China, approximately 27°N, 107°E], according to the original description; however, the specific locus remains unknown. Subsequently, this species has been reported from multiple localities in central, eastern, and southern China (Zhao et al. 1998; Chen et al. 2006; Guo and Deng 2006). However, based on voucher specimens and molecular data from this study, *P. boulengeri* is currently only within Chongqing, Hunan, Guizhou, Hubei, and Sichuan. The populations in southern Gansu and southern Shaanxi are temporarily classified as *P. boulengeri*. Previous records from the Dabie Mountains, at the junction of Anhui, Henan, and Hubei, should be assigned to *P. dabieshanensis* sp. nov. (Chen et al. 2006; Pan et al. 2014; this study), while previous records from southern Anhui, Jiangxi, and Zhejiang should be assigned to *P. orientalis* sp. nov. (this study).

***Pareas dabieshanensis* Zhang, Pan & Zhang, sp. nov.**

https://zoobank.org/C4F4089A-7A85-44E7-B8D9-C4747DA54D72

Pareas boulengeri (Chen et al. 2006; Pan et al. 2014). Chresonymy.

Type materials. ***Holotype*:** • An adult male (Fig. 4, AHU2024042601) was collected from the Tianma

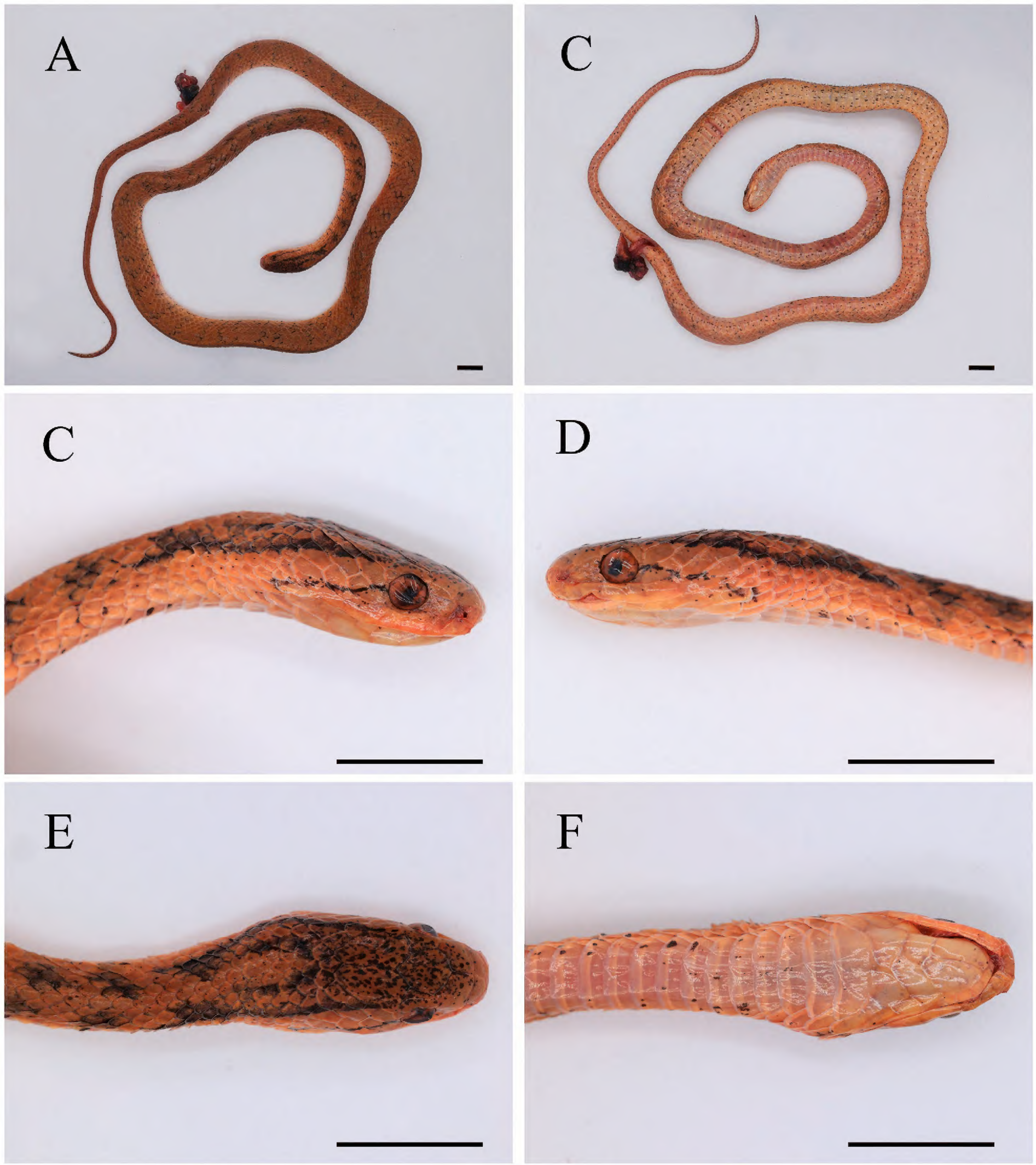

Figure 4. *Pareas dabieshanensis* sp. nov. in preservative (AHU2024042601). **A.** Dorsal view; **B.** Ventral view; **C.** Right lateral view of the head; **D.** Left lateral view of the head; **E.** Ventral view of the head; **F.** Dorsal view of the head. Scale bars: 10 mm.

National Nature Reserve (31.2250°N, 115.6831°E; elevation 807 m a.s.l.) in Jinzhai County, Luan City, Anhui Province, China, by Tao Pan and Wen-gang Li on April 26, 2024.

***Paratypes*:** • One adult male specimen (AHU2014100801) was collected from the Yaoluoping National Nature Reserve in Yuexi County, Anqing City, Anhui Province, China, by Tao Pan on October 08, 2014. • One adult male specimen (AHU2021050201) was collected from the Taiyang Township in Huoshan County, Luan City, Anhui Province, China, by Caiwen Zhang on May 02, 2021.

Etymology. *Pareas dabieshanensis* sp. nov. refers to the distribution of the new species in the Dabie Mountains. We recommend designating this new species Dabie Mountains Slug-eating Snake and 大别山钝头蛇 (Dà Bié Shān Dùn Tóu Shé).

Diagnosis. *Pareas dabieshanensis* sp. nov. is distinguished from its congeners by several morphological characteristics (Table 2): (1) medium body size (TL 443–

517 mm, n = 3 males); (2) yellow–brown body featuring numerous irregular black horizontal stripes; (3) the length of the suture between the internasals is subequal to that between the prefrontals, with the prefrontal bordering the orbit; (4) the frontal is subhexagonal to diamond-shaped, with its lateral sides converging posteriorly; (5) the anterior pair of chin shields is longer than broad; the loreal scale partially borders the orbit; (6) the prefrontal contacts the eye, and there are two subocular scales; (7) 7–8 supralabials and 9 infralabial scales; (8) 15-15-15 rows of dorsal scales, with mid-dorsal scales smooth, and the vertebral scale row is not enlarged; (9) 184–187 ventral scales and 68–74 subcaudals, divided, with a single cloacal plate; (10) prefrontal and postfrontal bones do not exhibit contact, asymmetric teeth number in maxilla, palatine, pterygoid, and dentary bones (MX 5/5, PAL 3/3, PT10–11/9–11, DT 16–18/20); (11) dorsal surface of the head exhibits a dense arrangement of small, black spots; three distinct black vertical stripes on the lateral aspect of the head, which do not converge; the central horizontal stripe, posterior to the supraorbital scales, extends posteriorly toward the neck; additionally, a horizontal stripe posterior to the eyes terminates at the posterior margin of the head; two black horizontal stripes are in the supraocular and postocular regions, extending only to the posterior margin of the head.

Holotype description. An adult male with a total length of 506 mm (SVL 398 mm, TaL 108 mm); relatively short tail (TaL/TL ratio 0.21); body slender, slightly compressed; head distinct from neck, snout wide and blunt, projecting beyond lower jaw; head elongate, clearly distinct from neck; snout round in dorsal view; eye slightly enlarged, pupil vertical and slightly elliptical; rostral approximately as wide as high, slightly visible from above; nasal undivided; internasal elongated; prefrontal, approximately trapezoidal, bordering orbits; frontal shield-shaped, slightly longer than wide; parietals large, longer than wide, gradual narrowing posteriorly, median suture approximately equal to length of frontal; one loreal, in contact with eye; two subocular scales, the anterior scale is diminutive, and the posterior scale is fused with the postocular scale, extending anteriorly beneath the eyes; temporals 2+3/2+3; 7/8 supralabial scales; 9/9 infralabials; 3 chin-shield pairs; dorsal scales exhibit a smooth texture and are arranged in 15 rows along the body, while the dorsal scale does not exhibit enlargement; 190 ventral scales; 70 subcaudals scales, paired; single cloacal plate. Prefrontal and postfrontal bones do not exhibit contact, asymmetric teeth number in maxilla, palatine, pterygoid, and dentary bones (MX 5/5, PAL 3/3, PT10/9, DT 18/21).

Coloration in life. Dorsal surface of the head exhibits a dense arrangement of small, black spots; three distinct black vertical stripes appear on the lateral aspect of the head and do not converge; the central horizontal stripe, posterior to the supraorbital scales, extends posteriorly toward the neck. A horizontal stripe posterior to the eyes terminates at the posterior margin of the head. Furthermore, two black horizontal stripes in the supraocular and postocular regions extend only to the posterior margin of the head. The dorsal surface is further distinguished by a yellowish-brown coloration featuring 47 irregular and discontinuous black horizontal stripes. In contrast, the ventral side exhibits a grayish-white coloration, adorned with scattered fine black spots.

Coloration in preservative. In its preserved form (Fig. 4), the specimen's coloration resembles its living appearance. However, the once yellowish–red dorsal surfaces of the head and body fade to a pinkish–brown,

Table 2. Comparisons of morphometric and scalation data for *Pareas boulengeri*, *P. dabieshanensis* sp. nov., and *P. orientalis* sp. nov. Measurements in mm. For a list of abbreviations, please refer to the Materials and Methods section.

Characters	*Pareas boulengeri* (n = 9)	*P. dabieshanensis* sp. nov. (n = 3)	*P. orientalis* sp. nov. (n = 9)
SVL	250–464	346–413	247–412
TaL	58–107	97–108	64–112
TL	308–566	443–517	311–524
TaL/TL	0.18–0.23	0.20–0.22	0.19–0.21
HL	12.30–20.79	15.9–19.48	12.72–19.24
HW	5.22–10.37	6.14–9.01	5.48–9.11
ED	2.41–3.27	2.53–2.87	2.27–3.1
ASR	15	15	15
MSR	15	15	15
PSR	15	15	15
VSE	0	0	0
KMD	0	1	0
VEN	175–188	184–187	175–187
SC	57–66	68–74	69–75
CP	entire	entire	entire
SL	7–8	7–8	7–8
IL	9	9	9
At	2	2	2
Pt	3	3	3
Preoc	0	0	1
SoO	Fused	2	Fused
PoO	Fused	Fused	Fused
LOR	1	1	1

with a notable reduction in vibrancy. The black stripes along the sides of the body and tail remain visible, preserving their contrast despite the fading in other areas. The pinkish–yellow belly and ventral portion of the head and tail also lighten to a pinkish–white. Moreover, the iris becomes grayish-black, while the pupil becomes white, reflecting additional changes in pigmentation due to the preservation process.

Variation. The three adult male specimens exhibited nearly identical morphological characteristics. The fundamental statistics related to the morphological measurements are presented in Suppl. material 1: tables S2, S3. The number of posterior temporals ranged from two to three. The number of vertical black stripes on each side of the body ranged from 48 to 53, while the iris color in the paratypes varied from reddish-yellow to yellow.

Distribution and habitat. Based on the existing distribution data, it is speculated that this species is mainly distributed in the Dabie Mountain area at the junction of

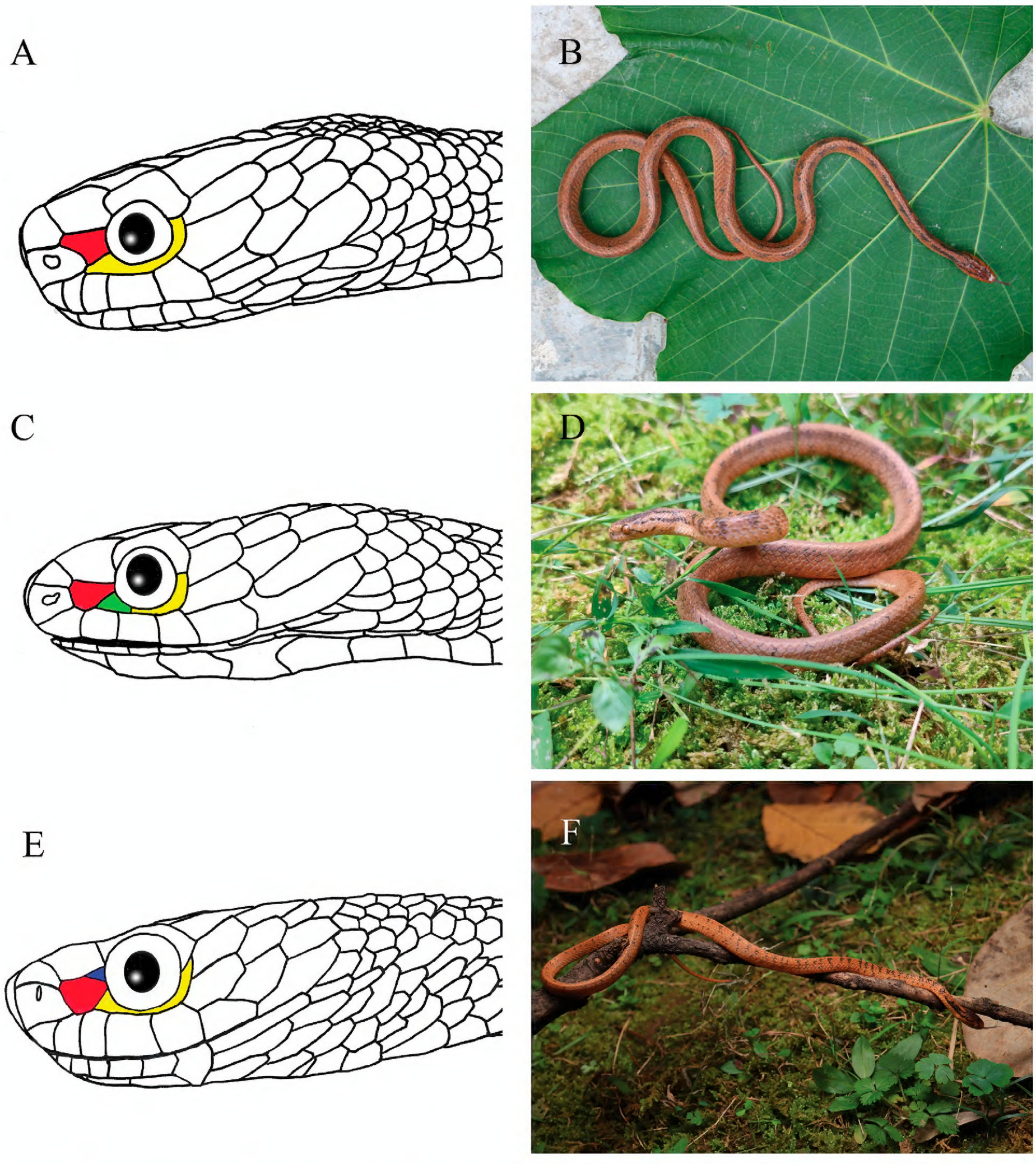

Figure 5. Comparative analysis of head scaling. Specimens include. **A.** *Pareas boulengeri* (LPSSC2024070502); **B.** A living specimen (GZNU2018052302); **C.** The holotype of *P. dabieshanensis* sp. nov. (AHU2024051501); **D.** A living specimen (AHU2021050201); **E.** The holotype of *P. orientalis* sp. nov. (AHU2024051501); and **F.** A living specimen (AHU2024051502). Photos by Cai-wen Zhang, Shan Shen, and Tao Luo.

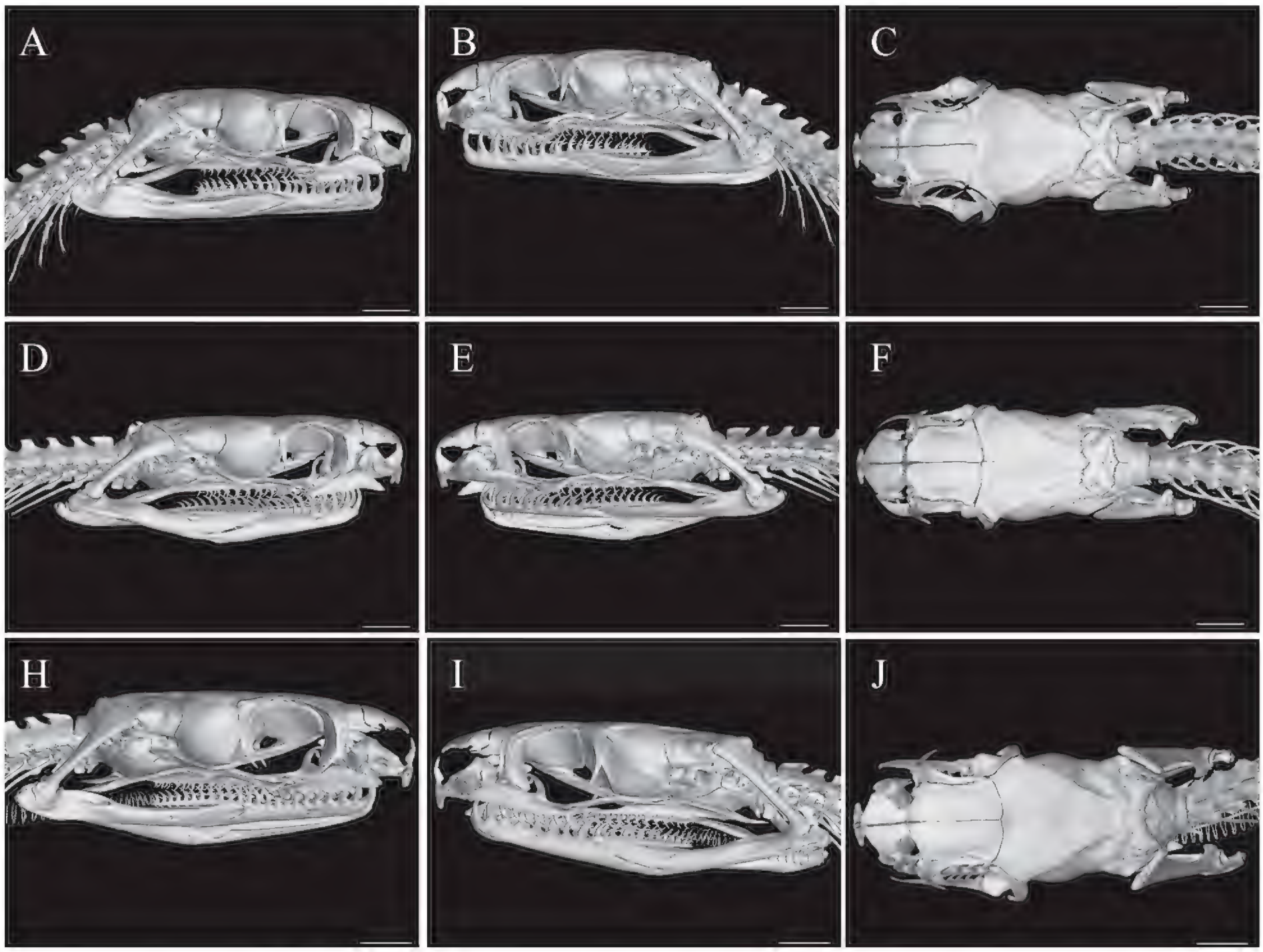

Figure 6. Three-dimensional model of the skull of *Pareas boulengeri*, *P. dabieshanensis* sp. nov., and *P. orientalis* sp. nov. Left, right lateral view; middle, left lateral view; right, dorsal view. **A–C.** *Pareas boulengeri* (LPSSY2021070801); **D–F.** The holotype of *P. dabieshanensis* sp. nov. (AHU2024051501); **H–J.** The holotype of *P. orientalis* sp. nov. (AHU2024051501). Implemented by Cai-wen Zhang and Jing-song Shi. Scale bars: 2 mm.

Anhui, Henan, and Hubei Province (Fig. 1). It inhabits mountainous regions, frequently residing near low shrubs adjacent to streams in low-altitude areas, and primarily feeds on slugs and snails.

Comparison. Comparisons between the new species and its congeners are summarized in Table 2. *Pareas dabieshanensis* sp. nov. was previously classified as *P. boulengeri*. However, this newly identified species can be differentiated from *P. boulengeri* in southwest China based on a higher number of subcaudal scales (68–74 vs. 57–66), two subocular scales (vs. one and fused suboculars with postoculars) (Fig. 5), and prefrontal and postfrontal bones do not exhibit contact (vs. contact) (Fig. 6).

Pareas dabieshanensis sp. nov. can be distinguished from *P. andersonii*, *P. macularius*, *P. margaritophorus*, and *P. modestus* by its yellow–brown dorsum featuring irregular dark bands (vs. uniform grey to black to dark coloration with bicolored spots), the loreal contacting the eye (vs. the loreal not contacting the eye), a greater number of ventral scales (184–187 vs. 141–162, 151–173, 133–160, or 151–159, respectively), and a greater number of subcaudals (68–74 vs. 35–47, 57–66, 35–54, or 35–46, respectively).

Pareas dabieshanensis sp. nov. can be easily distinguished from *P. abros*, *P. atayal*, *P. baiseensis*, *P. berdmorei*, *P. carinatus*, *P. formosensis*, *P. geminatus*, *P. guanyinshanensis*, *P. hamptoni*, *P. kaduri*, *P. komaii*, *P. kuznetsovorum*, *P. niger*, *P. nuchalis*, *P. temporalis*, *P. tigerinus*, and *P. xuelinensis* by the presence of a loreal scale in contact with the eye (vs. the loreal scale not contacting the eye).

Pareas dabieshanensis sp. nov. can be distinguished from *P. chinensis* by the absence of preoculars (vs. one preocular), two subocular scales, one of which is fused with the postocular scale (vs. not fused), dorsal scales not enlarged (vs. one vertebral scale row enlarged), and dorsal scale smooth at midbody (vs. three keeled dorsal scale rows at midbody).

Pareas dabieshanensis sp. nov. differs from *Pareas dulongjiangensis* by lacking preoculars (vs. one preocular), having two subocular scales, one of which is fused with the postocular scale (vs. only one and suboculars fused with postoculars), dorsal scales not enlarged (vs. three vertebral scale rows enlarged), and a dorsal scale smooth at midbody (vs. five keeled dorsal scale rows at midbody).

Pareas dabieshanensis sp. nov. can be easily distinguished from *Pareas iwasakii* by the absence of preoculars (vs. one preocular), having postoculars fused with suboculars

(vs. distinct and separated postoculars and suboculars), fewer ventral scales (184–187 vs. 190–193), fewer subcaudal scales (68–74 vs. 76–84), dorsal scales not enlarged (vs. one vertebral scale row enlarged), and dorsal scale smooth at midbody (vs. 5–7 keeled dorsal scale rows at midbody).

Pareas dabieshanensis sp. nov. differs from *P. monticola* with more infralabial scales (9 vs. 7–8) and a smooth dorsal scale at midbody (vs. 1–3 keeled dorsal scale rows at midbody).

Pareas dabieshanensis sp. nov. differs from *P. nigriceps* by having more infralabial scales (9 vs. 7), lacking preoculars (vs. one preocular), having two anterior temporals (vs. one anterior temporal), two subocular scales, one of which is fused with the postocular scale (vs. only one and suboculars fused with postoculars), dorsal scales that are not enlarged (vs. one enlarged vertebral scale row), and a smooth dorsal scale at midbody (vs. 9 keeled dorsal scale rows at midbody).

Pareas dabieshanensis sp. nov. differs from *P. stanleyi* by having more infralabial scales (9 vs. 7–8), postoculars fused with suboculars (vs. distinct and separated postocular and subocular), more ventral scales (184–187 vs. 151–160), more subcaudal scales (68–74 vs. 48–64), and a smooth dorsal scale at midbody (13 keeled dorsal scale rows at midbody).

Pareas dabieshanensis sp. nov. differs from *P. victorianus* by having more infralabial scales (9 vs. 6–7), two subocular scales, one of which is fused with the postocular scale (vs. only one and subocular fused with postocular), more ventral scales (184–187 vs. 164), more subcaudal scales (68–74 vs. 58), dorsal scales not enlarged (vs. one enlarged vertebral scale row), and a smooth dorsal scale at midbody (vs. eight keeled dorsal scale rows at midbody).

Pareas dabieshanensis sp. nov. differs from *P. vindumi* by having more supralabials (7–8 vs. 6), more infralabials (9 vs. 6), two subocular scales, one of which is fused with the postocular scale (vs. only one and subocular fused with postocular), more ventral scales (184–187 vs. 178), and more subcaudal scales (68–74 vs. 61).

Pareas dabieshanensis sp. nov. differs from *P. yunnanensis* by having more infralabials (9 vs. 6), lacking preoculars (vs. 1–2 preoculars), having two subocular scales, one of which is fused with the postocular scale (vs. only one and subocular fused with postocular), more ventral scales (184–187 vs. 169–175), more subcaudal scales (68–74 vs. 59–65), dorsal scales not enlarged (vs. one enlarged vertebral scale row), and a smooth dorsal scale at the midbody (vs. 5–7 keeled dorsal scale rows at midbody).

Remarks. In 1974, the Sichuan Institute of Biology first discovered *Pareas chinensis* in the Dabie Mountains of Anhui Province. The amphibian and reptile fauna of Anhui suggest that this species is also present in Qianshan and Huoshan County (Chen 1991). Additionally, Chen et al. (2006) identified *P. boulengeri* for the first time in the Jingangtai National Nature Reserve, in the Dabie Mountains of Henan Province. Pan et al. (2014) further confirmed the presence of this species in the Dabie Mountains of Anhui and reclassified *P. chinensis* as *P. boulengeri*. This species has been detected in multiple localities within the Dabie Mountains (Pan et al. 2014; this study). Furthermore, *P. dabieshanensis* sp. nov. is likely found in eastern Hubei, which is geographically connected to western Anhui; however, further confirmation is required through additional voucher specimens.

Pareas orientalis Zhang, Pan & Zhang, sp. nov.

https://zoobank.org/52FEBF33-9BBA-4636-BC3A-A9538CF46E78

Pareas boulengeri (Chen 1991; Zhao et al. 1998). Chresonymy.

Etymology. *Pareas orientalis* sp. nov. refers to the new species in eastern China. We recommend designating this new species the Eastern China slug-eating snake and 华东钝头蛇 (Huá Dōng Dùn Tóu Shé).

Type materials. ***Holotype*:** • An adult male (Fig. 7, AHU2024051501) from the Fengteng Village (29.5992°N, 117.9743°E; elevation 249 m a.s.l.), Xiuning County, Huangshan City, Anhui Province, China, was collected by Lei Yu and Muyao Zhang on 15 May 2024.

***Paratypes*:** Eight specimens (3 females and 5 males) were collected from Huangshan City and its surrounding areas. • One adult male specimen (AHU2024051502) was collected on the same day and at the same location as the holotype. Additionally, • two females (AHU2015062201, AHU2015082001) and three males (AHU2020061201, AHU2024072201, AHU2024072202) were collected in Huangshan City. Furthermore, • one adult female specimen (AHU2019071201) was obtained from Jing County, Huangshan City, • one adult male (AHU2021101501) was collected from Chunan County, Hangzhou City, Zhejiang Province.

Diagnosis. *Pareas orientalis* sp. nov. can be distinguished from its congeners based on the following morphological characteristics: (1) medium body size (TL 311–452 mm, n = 3 females; 420–524 mm, n = 6 males); (2) yellow–brown body coloration with many irregular black horizontal stripes; (3) the length of suture between internasals subequal to that between the prefrontals, with prefrontal bordering orbit; (4) the frontal subhexagonal to diamond-shaped with lateral sides converging posteriorly; (5) one subocular, one preocular, one loreal, and only tip bordering eye; (6) the prefrontal contacts the eye, and there one subocular scale fused with postocular scale; (7) 7–8 supralabial scales, 9 infralabial scales; (8) rows of 15-15-15 dorsal scales, three rows of mid-dorsal scales slightly keeled at the midline, median vertebral scale row not enlarged; (9) 175–187 ventrals, 69–75 subcaudals, divided, with a single cloacal plate; (10) prefrontal and postfrontal bones do not exhibit contact, asymmetric teeth number in maxilla, palatine, pterygoid, and dentary bones (MX 6–7/5–6, PAL 3/3–4, PT12–14/12–13, DT 17–19/21–23); (11) dorsal surface of the head exhibits a dense arrangement of small, black spots; two black longitudinal stripes extend posteriorly, behind the parietal and supraocular scales, converging into a prominent black stripe in the neck region; a slender black horizontal line is present on the lateral aspect of the head, posterior to the eye and extending toward the corner of the mouth.

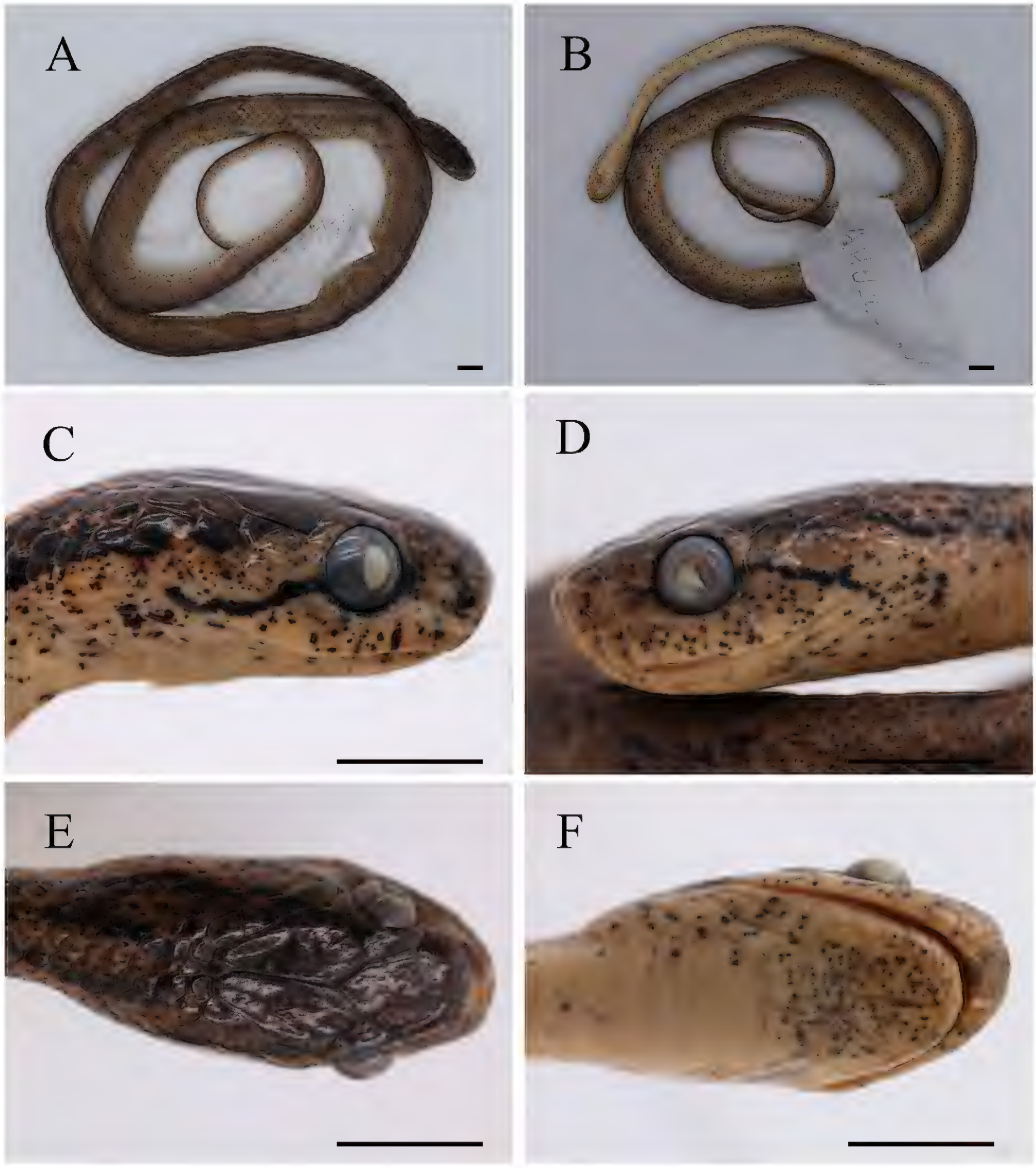

Figure 7. *Pareas orientalis* sp. nov. in preservative (AHU2024051501). **A.** Dorsal view; **B.** Ventral view; **C.** Right lateral view of the head; **D.** Left lateral view of the head; **E.** Ventral view of the head; **F.** Dorsal view of the head. Scale bars: 10 mm.

Holotype description. An adult male with a 515 mm total length (SVL 405 mm, TaL 110 mm); relatively short tail (TaL/TL ratio 0.21); body slender, slightly compressed; head distinct from neck with a wide and blunt snout, projecting beyond lower jaw; head elongate, clearly distinct from neck; snout round in dorsal view; eye slightly enlarged, pupil vertical and slightly elliptical; rostral approximately as wide as high, slightly visible from above; nasal undivided; internasal elongated; prefrontal, approximately trapezoidal, bordering orbits; frontal shield-shaped, slightly longer than wide; parietals large, longer than wide, gradually narrows posteriorly, median suture approximately equal to length of frontal; one loreal, in contact with eye; one triangular preocular scale; one subocular scale that converges with the postocular scale, extending from the posterior aspect of the eye to the ventral corner of the eye; temporals 2+3/2+3; 8/8 supralabial scales; 9/9 infralabials; three chin-shield pairs; dorsal scales are mostly smooth, with three rows of mid-dorsal scales slightly keeled at the midline and arranged in 15 rows, while dorsal scales are not enlarged; 182 ventral scales; 72 subcaudal scales, paired; single cloacal plate. Prefrontal and postfrontal bones do not exhibit contact, asymmetric teeth number in maxilla,

palatine, pterygoid, and dentary bones (MX 7/6, PAL 3/4, PT14/12, DT . 8/23).

Coloration in life. Dorsal surface of the head exhibits a dense arrangement of small, black spots; two black longitudinal stripes extend posteriorly, behind the parietal and supraocular scales, converging into a prominent black stripe in the neck region. A slender black horizontal line is on the lateral aspect of the head, posterior to the eye and extending toward the corner of the mouth. The dorsal surface is distinguished by a yellowish-brown coloration featuring 52 irregular and discontinuous black horizontal stripes. In contrast, the ventral side displays a grayish-white coloration, embellished with scattered fine black spots.

Coloration in preservative. In its preserved state, the specimen's coloration resembles that of its living condition. The yellowish–red dorsal surfaces of the head and body fade to a pinkish–brown hue, indicating a significant loss of vibrant pigmentation. Notably, the black stripes along the sides of the body and tail remain distinct, maintaining their contrast despite fading in other regions. The pinkish-yellow coloration of the belly and the ventral surfaces of the head and tail diminishes to a pinkish-white, suggesting further pigment degradation. Additionally, the iris transforms to a grayish-black, while the pupil becomes white, reflecting further changes in pigmentation attributable to the preservation process.

Variation. The nine specimens exhibited nearly identical morphological characteristics. The fundamental statistics for the morphological measurements are presented in Suppl. material 1: tables S2, S3. The quantity of posterior temporals ranged from two to three. The number of vertical black stripes on each side of the body ranged from 45 to 58, while the iris color in the paratypes varied from reddish-yellow to yellow.

Distribution and habitat. Based on the available distribution data, this species is hypothesized to be predominantly located in southern Anhui, southern Jiangsu, northern Jiangxi, and Zhejiang (Fig. 1). It inhabits mountainous regions, frequently residing near low shrubs adjacent to streams in low-altitude areas, and primarily feeds on slugs and snails.

Comparison. Comparisons between the new species and its congeners are summarized in Table 3. *Pareas orientalis* sp. nov. and *P. dabieshanensis* sp. nov. were previously classified as *P. boulengeri*. However, *P. orientalis* sp. nov. exhibits distinct morphological characteristics. *Pareas orientalis* sp. nov. can be differentiated from *P. dabieshanensis* sp. nov. (Figs 5, 6) by the presence of one preocular scale (vs. no preocular scale), one subocular fused with the postocular (vs. two subocular scales, one of which is fused with the postocular scale), and three rows of middorsal scales keeled at the midline (vs. smooth at midbody), fewer teeth number in maxilla bone (MX 5–7 vs. 5), and more teeth number in pterygoid bone (PT12–14 vs. 9–11). The distinction between *P. orientalis* sp. nov. and true *P. boulengeri* is characterized by one preocular scale (vs. no such scale), more subcaudals (69–75 vs. 57–66), and fewer teeth number in maxilla bone (MX 5–7 vs. 4–5).

Given that *P. orientalis* sp. nov. and *P. dabieshanensis* sp. nov. exhibit morphological similarities, with most morphological features relatively comparable and their body colors largely indistinguishable, the primary differences lie in the presence or absence of preocular scales, the number of subocular scales, and the presence of keeled mid-dorsal scales at the midline of the body. As *P. dabieshanensis* sp. nov. was extensively compared with other species in the preceding section of the article, redundant elements have been excluded here.

Pareas orientalis sp. nov. can be distinguished from *P. andersonii*, *P. macularius*, *P. margaritophorus*, and *P. modestus* by a yellow–brown dorsum (yellow–brown vs. grayish). *P. orientalis* sp. nov. can be distinguished from *P. abros*, *P. atayal*, *P. baiseensis*, *P. berdmorei*, *P. carinatus*, *P. formosensis*, *P. geminatus*, *P. guanyinshanensis*, *P. hamptoni*, *P. kaduri*, *P. komaii*, *P. kuznetsovorum*, *P. niger*, *P. nuchalis*, *P. temporalis*, *P. tigerinus*, and *P. xuelinensis* by the presence of a loreal scale in contact with the eye (vs. the loreal scale not contacting the eye).

Pareas orientalis sp. nov. can be distinguished from *P. chinensis*, *P. iwasakii*, *P. monticola*, and *P. stanleyi* by suboculars fused with postoculars (vs. separated).

Pareas orientalis sp. nov. can be distinguished from *Pareas dulongjiangensis*, *P. victorianus*, and *P. vindumi* by the presence of one preocular scale (vs. no preocular scale).

Pareas orientalis sp. nov. differs from *P. nigriceps* and *P. yunnanensis* by having more infralabial scales (9 vs. 6–8).

Discussion

The phylogenetic analysis conducted by Poyarkov et al. (2022) supports the classification of the genus *Pareas* into six distinct species groups: *P. carinatus*, *P. nuchalis*, *P. chinensis*, *P. hamptoni*, *P. monticola*, and *P. margaritophorus*. The findings of the current study indicate that *P. boulengeri*, *P. dabieshanensis* sp. nov., and *P. orientalis* sp. nov. are members of the *P. chinensis* species group. Notably, *P. dabieshanensis* sp. nov. possesses two subocular scales, aligning with the characteristics of *P. baiseensis* but contradicting the diagnostic features attributed to the subgenus *Eberhardtia*, as outlined by Poyarkov et al. (2022). Consequently, as proposed by Gong et al. (2023), we recommend revising the diagnostic parameters by removing the single thin elongated subocular characteristic.

Pareas boulengeri was previously believed to have a broad distribution across various regions in China, encompassing 16 provinces: Anhui, Chongqing, Henan, Hunan, Gansu, Guangdong, Guangxi, Guizhou, Fujian, Jiangsu, Jiangxi, Shaanxi, Sichuan, Yunnan, and Zhejiang (Zhao et al. 1998; Chen et al. 2006; Guo and Deng 2006; Zhao 2006). The *Pareas* genus, characterized by its ancient origins and limited migratory capabilities, exhibits a notable degree of limited variation in morphological traits, with relatively

Table 3. The diagnostic features of scalation and dorsal coloration of *Pareas dabieshanensis* sp. nov. and *Pareas orientalis* sp. nov. are compared with those of the currently recognized species within the genus *Pareas*. Exceptional values are indicated in parentheses. The following abbreviations are utilized: TL max. = maximum total length; SPL = supralabials; IFL = infralabials; Preoc = number of preoculars; SoO = number of sunoculars; PoO = number of postoculars; TEP = number of temporals; Loreal = loreal-eye contact; DSR = dorsal scale rows; Ven = ventral scales; Sc = subcaudals; enlarged = median vertebral scale row slightly enlarged; keeled = median scale rows slightly keeled; color = dorsal coloration.

ID	Species	max. TL	SPL	IFL	Preoc	SoO	PoO	TEP	Loreal	DSR	VEN	SC	enlarged	keeled	color	source
1	*P. dabieshanensis* **sp. nov.**	517	7–8	9	0	2	Fused	2+3	yes	15	184–187	68–74	0	0	yellow-brown	1
2	*P. orientalis* **sp. nov.**	524	7–8	9	1	Fused	Fused	2+2 or 2+3	yes	15	175–187	69–75	0	3	yellow-brown	1
3	*P. abros*	565	9	8–9	1	3	2	3+3	no	15	180–184	83–95	1	9–11	yellow-brown	2
4	*P. andersonii*	481	9	7–8	0	1	1	2	no	15	141–162	35–47	0	5–9	grayish	3
5	*P. atayal*	560	9	7–9	1	Fused	Fused	2+3 or 2+4	no	15	174–188	71–77	2	7	yellow-brown	4
6	*P. baiseensis*	579	8	9	1	2–3	1	2 + 3 or 3 + 3	no	15	187–191	89–97	1	5	yellow-brown	5
7	*P. berdmorei*	770	9	7–9	1–2	1–3	0–2	3 + 4 or 3 + 3	no	15	162–187	57–89	1–3	3–13	yellow-brown	2
8	*P. boulengeri*	566	7–8	9	0	Fused	Fused	2+2 or 2+3	yes	15	175–188	57–66	0	0	yellow-brown	1
9	*P. carinatus*	610	7–9	7–9	2	1 or 2	2	2+3	no	15	172–183	66–89	3	9–13	yellow-brown	4, 8
10	*P. chinensis*	682	7–9	7–9	1	1	1	2+3	no or only tip	15	166–192	56–84	1	3	yellow-brown	6, 7, 8
11	*P. dulongjiangensis*	488	6—7	7—9	0	Fused	Fused	2+3 or 2+2	yes	15	182	76	3	5	yellow-brown	9
12	*P. formosensis*	617	7–8	7	1	1	1	2+3 or 2+2	no	15	163–181	70–80	3		yellow-brown	4, 8
13	*P. geminatus*	566	6–8	8	1	Fused	Fused	1–2	no	15	170–188	75-91	1	3–5	yellow-brown	8
14	*P. guanyinshanensis*	540	7–8	6–8	1	Fused	Fused	2+2 or 2+3 or 2+4	no	15	189–192	72–89	1	5	yellow-brown	9
15	*P. hamptoni*	483	7–8	6–9	1	1 or Fused	1 or Fused	1+2 or 2+3	no	15	185–195	91–99	1–3	5–9	yellow-brown	8
16	*P. iwasakii*	700	NA	9–11	1	1	1	3+4 or 2+3	yes	15	190–193	76–84	1	5–7	yellow-brown	4, 10, 11
17	*P. kaduri*	694	7	7	1	1	2	2+3	no	15	160–183	52–70	1	8	yellow-brown	12
18	*P. komaii*	600	7	7	1	1	1	2+3	no	15	162–182	60–76	3	9–13	yellow-brown	4, 11
19	*P. kuznetsovorum*	639	7	7–8	1	2	1	3+4	no	15	167	87	1	0	yellow-brown	2
20	*P. macularius*	517	7	6–8	1	1	1	2+3	no	15	151–173	39–53	0	5–11	grayish	8,19
21	*P. margaritophorus*	394	6–9	5–9	1	1	1	2+3	no	15	133–160	35–54	0	0	grayish	8,19
22	*P. modestus*	357	7	7	1	1	1	2+3	no	15	151–159	35–46	0	3–5	grayish	8,19
23	*P. monticola*	750	7–8	7–8	0	1	1	2+3	yes	15	178–199	69–90	1–3	0	yellow-brown	8,12
24	*P. niger*	585	6–7	8–9	1	Fused	Fused	2+3	no	15	167–173	54–61	3	3–9	yellow-brown	13
25	*P. nigriceps*	520	7	7	1	Fused	Fused	1+2 or 1+3	yes	15	175–184	73–77	1	9	brownish-black	8,14
26	*P. nuchalis*	678	7–8	6–8	1	1–3	1–2	3 + 4 or 3 + 3	no	15	201–220	102–120	1–3	0	brown	8
27	*P. stanleyi*	650	7–8	7–8	0	1	1	2 + 2 or 2 + 3	yes	15	151–160	48–64	0	13	yellow-brown	8,13
28	*P. temporalis*	578	8–9	8–9	2–3	2	2–3	4+3	no	15	191	92	3	all	yellow-brown	15
29	*P. tigerinus*	543	7	7	1	Fused	Fused	1+1 or 1+2	no	15	160–171	62-64	1	3–5	yellow-brown	16
30	*P. victorianus*	487	7	6–7	0	Fused	Fused	2+3	yes	15	164	58	1	8	yellow-brown	17
31	*P. vindumi*	657	6	6	0	Fused	Fused	2+3	yes	15	178	61	0	0	yellow-brown	17
32	*P. xuelinensis*	576	7	7—9	1	Fused	Fused	2 + 2 or 2 + 3	no	15	182–188	87–93	0	0–5	yellow-brown	18
33	*P. yunnanensis*	586	6–8	6–8	1–2	Fused	Fused	1+2 or 2+2 or 2+3	yes	15	169–175	59–65	1	5–7	yellow-brown	17

Note: Sources are denoted as follows: 1 = This study; 2 = Poyarkov et al. (2022); 3 = Vogel et al. (2020); 4 = You et al. (2015); 5 = Gong et al. (2023); 6 = Jiang (2004); 7 = Vogel (2015); 8 = Ding et al. (2020); 9 = Liu et al. (2024); 10 = Ota et al. (1997); 11 = Oskyrko et al. (2024); 12 = Bhosale et al. (2020); 13 = Wang et al. (2020); 14 = Guo and Zhao (2004); 15 = Le et al. (2021); 16 = Liu et al. (2023a); 17 = Vogel et al. (2020); 18 = Liu and Rao (2021).

minor distinctions among species, particularly in coloration and scale number (You et al. 2015; Poyarkov et al. 2022). Consequently, species once classified as *P. boulengeri* may have been misidentified due to the close morphological similarities among related species. Therefore, further molecular investigations of *P. boulengeri*, which is currently identified in the provinces of Gansu, Guangdong, Fujian, and Shaanxi, are crucial for clarifying existing taxonomic ambiguities.

Additionally, it is important to address the three species sites depicted in Fig. 1 that lie outside the suspected distribution ranges of the identified species. Originally classified as *P. boulengeri*, these sites were not categorized into any of the three species in this study due to the absence of mitochondrial gene sequences from local specimens. Given the subtle morphological differences among *Pareas* species, these records may represent misidentifications of *Pareas* taxa. However, they also present the possibility of being *P. orientalis* or even an undescribed species, particularly since their geographic locations fall outside the currently recognized distribution boundaries. This discrepancy underscores the need for cautious interpretation of distributional data, as misidentifications in GBIF uploads could potentially obscure the true ecological niche of these species. We encourage future surveys to prioritize field validation of these outlying records through comprehensive sampling, morphological re-examination, and genetic sequencing. Such efforts will be critical for determining whether these sites represent range extensions, misclassifications, or the presence of cryptic species—thereby refining our understanding of *Pareas* distribution dynamics and enabling more accurate delineation of species ranges in subsequent studies.

Identifying *P. dabieshanensis* sp. nov. and *P. orientalis* sp. nov. has increased the total recognized *Pareas* species to 33, with 27 documented in China (Uetz et al. 2025). Currently, three species belonging to the genus *Pareas* have been identified in Anhui Province: *P. chinensis*, *P. dabieshanensis* sp. nov., and *P. orientalis* sp. nov. (Chen 1991; Pan et al. 2014). In Anhui Province, our collections included *P. dabieshanensis* sp. nov. and *P. orientalis* sp. nov., but not *P. chinensis*. This suggests that previous records of *P. chinensis* in Anhui may have resulted from misidentification of *P. orientalis* sp. nov. Further survey efforts are necessary to enhance our understanding of the distribution of blunt-headed snakes in Anhui Province and to elucidate the diversity of the *Pareas* genus in this area.

However, the results of this study indicate that *Pareas boulengeri* is restricted to the provinces of Guizhou, Sichuan, Hubei, Yunnan, and Guangxi in southwestern China, while *P. dabieshanensis* sp. nov. is confined to the Dabie Mountain region in central China. Concurrently, *P. orientalis* sp. nov. occurs in southern Anhui, southern Jiangsu, northern Jiangxi, and Zhejiang in eastern China. Notably, the distribution ranges of these three species do not overlap. It is particularly noteworthy that *P. dabieshanensis* sp. nov. and *P. orientalis* sp. nov. are separated solely by the Yangtze River. Previous research has established that the river, as a significant hydrological system, acts as a natural barrier that has contributed to the evolutionary isolation of species (Carmichael et al. 2001; Wang et al. 2015; Zhang et al. 2023). Hence, the Yangtze River, as a natural barrier and ecological isolation zone, has had a profound impact on the evolution and diversity of species. Similar patterns have been observed in closely related species, such as *Achalinus dabieshanensis* and *A. huangjietangi*, which are geographically divided by the Yangtze River (Zhang et al. 2023), as well as *P. hamptoni* and *P. guanyinshanensis*, which are separated by the Red River (Liu et al. 2024). Consequently, the observed distribution pattern may be attributed to the distinctive topographic and climatic characteristics present on either side of the Yangtze River. Future research on the comparative phylogeography of these species could be conducted to investigate the underlying mechanisms of their formation.

On the other hand, studies on the asymmetric mandibular teeth of *Pareas* snakes and their mollusc prey have highlighted a novel aspect of the evolution of these snakes (You et al. 2015). Although the sample size is limited, preliminary evaluation of the dentition asymmetry index showed substantial variation among the specimens evaluated in this study (Suppl. material 1: table S3). Further studies on the correlation between dentition asymmetry and prey preference, using a larger sample size, will provide insight into dietary resource partitioning and niche differentiation between these species.

Scientific field survey permission information

This study was approved by the Institutional Animal Care and Use Committee of the School of Life Sciences, Anhui University (project number: IACUC (AHU)-2023-060; approval date: 17 November 2022). The management offices of the Yaoluoping National and Wanfoshan Provincial Nature Reserves granted permission for field surveys and species collection in the Dabie Mountains.

Funding

This study was supported by the Comprehensive Monitoring Station for National Ecological Quality in the Dabie Mountains (Forest): Ecological Monitoring for the Years 2024–2025 (ZF2024-18-1376).

Acknowledgments

We would like to express our sincere gratitude to Dr. Jing-song Shi at the Institute of Vertebrate Paleontology and Paleoanthropology (IVPP), Chinese Academy of Sciences, for his invaluable contributions. We also

extend our appreciation to Dr. Zhong Chen of Anhui University for providing two snake specimens that were essential to our study. Additionally, we would like to thank Professor Chen Hong from Liupanshui University for supplying three snake specimens. Furthermore, we wish to acknowledge the significant support of Wen-gang Li, Mu-yao Zhang, Fei Hong, and Chang-ting Lan throughout this research. We are also grateful for the assistance provided by Jun Ding and Laisheng Huang from the Wanfoshan Provincial Nature Reserve during the fieldwork. Our acknowledgments further extend to Jun Chu, Yong Chu, Xinjian Wang, and Xinxiang Li from the Yaoluoping National Nature Reserve, as well as Faguang Pu from the Tianma National Nature Reserve, for their contributions.

References

Akaike H (1974) A new look at the statistical model identification. IEEE Transactions on Automatic Control 19(6): 716–723. https://doi.org/10.1109/TAC.1974.1100705

Bhosale H, Phansalkar P, Sawant M, Gowande G, Patel H, Mirza ZA (2020) A new species of snail-eating snakes of the genus *Pareas* Wagler, 1830 (Reptilia, Serpentes) from eastern Himalayas, India. European Journal of Taxonomy 729(1): 54–73. https://doi.org/10.5852/ejt.2020.729.1191

Boulenger GA (1900) Descriptions of new reptiles and batrachians from Borneo. Proceedings of the Zoological Society of London 69(2): 182–187. https://doi.org/10.1111/j.1096-3642.1890.tb01716.x

Boulenger GA (1905) Descriptions of two new snakes from upper Burma. Journal of the Bombay Natural History Society 16: 235–236. https://doi.org/10.1080/03745480509443665

Boulenger GA (1914) Descriptions of new species of snakes in the collection of the British Museum. Annals & Magazine of Natural History 14(84): 482–485. https://doi.org/10.1080/00222931408693606

Carmichael LE, Nagy JA, Larter NC, Strobeck C (2001) Prey specialization may influence patterns of gene flow in wolves of the Canadian Northwest. Molecular Ecology 10: 2787–2798. https://doi.org/10.1046/j.0962-1083.2001.01408.x

Chen BH (1991) The Amphibian and Reptilian Fauna of Anhui. Anhui Science and Technology Publishing House, Hefei. [in Chinese]

Chen XH, Zhu MW, Hou MG, Zhai WY (2006) A new record of Colubridae from Henan Province: *Pareas boulengeri*. Sichuan Journal of Zoology 25(2): 269. [in Chinese]

Ding L, Chen Z, Suwannapoom C, Nguyen TV, Poyarkov NA, Vogel G (2020) A new species of the *Pareas hamptoni* complex (Squamata Serpentes, Pareidae) from the Golden Triangle. Taprobanica 9: 174–193. https://doi.org/10.47605/tapro.v9i2.230

Dowling HG (1951) A proposed standard system of counting ventrals in snakes. British Journal of Herpetology 1: 97–99.

Eriksson J, Hohmann G, Boesch C, Vigilant L (2004) Rivers influence the population genetic structure of bonobos (*Pan paniscus*). Molecular Ecology 13(11): 3425–3435. https://doi.org/10.1111/j.1365-294X.2004.02332.x

Gong Y, Wu J, Huang S, Xu Y, Yang D, Liu Y, Liang S, Lee P (2023) A New Species of *Pareas* (Squamata, Pareidae) from Guangxi Province, China. Animals 13: 2233. https://doi.org/10.3390/ani13132233

Guindon S, Gascuel O (2003) A simple, fast, and accurate algorithm to estimate large phylogenies by maximum likelihood. Systematic Biology 52(5): 696–704. https://doi.org/10.1080/10635150390235520

Guo KJ, Deng XJ (2006) A new record of snakes in Hunan Province-Flat-scaled *Pareas boulengeri*. Sichuan Journal of Zoology 25(2): 270. [in Chinese]

Guo P, Zhao EM (2004) *Pareas stanleyi* – A record new to Sichuan, China and a key to the Chinese species. Asiatic Herpetological Research 10: 280–281.

Guo YH, Wu YK, He SP, Shi HT, Zhao EM (2011) Systematics and molecular phylogenetics of Asian snail-eating snakes (Pareatidae). Zootaxa 3001: 57–64. https://doi.org/10.11646/zootaxa.3001.1.4

Hall TA (1999) BioEdit: A user-friendly biological sequence alignment editor and analysis program for Windows 95/98/NT. Nucleic Acids Symposium Series 41(41): 95–98.

Hu SQ, Zhao EM, Liu CC (1973) A survey of amphibians and reptiles in Kweichow province, including a herpetofaunal analysis. Acta Zoologica Sinica/Dong wu xue bao 19: 149–181.

Huang RY, Peng LF, Yang DC, Yong Z, Huang S (2020) Mitochondrial genome of the Boulenger's Slug-eating snake *Pareas boulengeri* (Serpentes: Pareidae). Mitochondrial DNA Part B. 5: 3161-3162. https://doi.org/10.1080/23802359.2020.1804471

Hoso M, Asami T, Hori M (2007) Right-handed snakes: Convergent evolution of asymmetry for functional specialization. Biology Letters 3: 169–172. https://doi.org/10.1098/rsbl.2006.0600

Jiang YM (2004) *Pareas chinensis* (Babour, 1912) should be a junior synonym of *Pareas formosensis* (Van Denburgh, 1909). Sichuan Journal of Zoology 23(3): 209–210. [in Chinese]

Katoh K, Standley DM (2013) MAFFT multiple sequence alignment software version 7: Improvements in performance and usability. Molecular Biology and Evolution 30(4): 772–780. https://doi.org/10.1093/molbev/mst010

Katoh K, Kuma K, Toh H, Miyata T (2005) MAFFT version 5: Improvement in accuracy of multiple sequence alignment. Nucleic Acids Research 33(2): 511–518. https://doi.org/10.1093/nar/gki198

Lawson R, Slowinski JB, Crother BI, Burbrink FT (2005) Phylogeny of the Colubroidea (Serpentes): New evidence from mitochondrial and nuclear genes. Molecular Phylogenetics and Evolution 37(2): 581–601. https://doi.org/10.1016/j.ympev.2005.07.016

Le DTT, Tran TG, Hoang HD, Stuart BL (2021) A new species of *Pareas* (Squamata, Pareidae) from southern Vietnam. Vertebrate Zoology 71: 439–451. https://doi.org/10.3897/vz.71.e70438

Li JN, Liang D, Wang YY, Guo P, Huang S, Zhang P (2020) A large-scale systematic framework of Chinese snakes based on a unified multilocus marker system. Molecular Phylogenetics and Evolution 148: 106807. https://doi.org/10.1016/j.ympev.2020.106807

Liu S, Rao DQ (2021) A new species of the genus *Pareas* (Squamata, Pareidae) from Yunnan, China. ZooKeys 1011: 121–138. https://doi.org/10.3897/zookeys.1011.59029

Liu S, Yang M, Rao J, Guo Y, Rao D (2023a) A New Species of *Pareas* Wagler, 1830 (Squamata, Pareidae) from Northwestern Yunnan, China. Taxonomy 3(2): 169–182. https://doi.org/10.3390/taxonomy3020013

Liu S, Zhang DR, Poyarkov NA, Hou M, Wu L, Rao DQ, Nguyen TV, Vogel G (2023b) Resurrection of *Pareas yunnanensis* (Vogt, 1922) with description of a new species of *Pareas* from Yunnan Province, China (Squamata, Pareidae). European Journal of Taxonomy 860(1): 1–26. https://doi.org/10.5852/ejt.2023.860.2045

Liu S, Mo M, Li M, Li B, Luo X, Rao DQ, Li S (2024) Description of a New Species of the *Pareas hamptoni* Complex from Yunnan, China, with Confirmation of *P. hamptoni* Sensu Stricto in China (Squamata, Pareidae). Animals 14(3): 421. https://doi.org/10.3390/ani14030421

Loredo AI, Wood PL, Quah ESH, Anuar S, Greer LF, Ahmad N, Grismer LL (2013) Cryptic speciation within *Asthenodipsas vertebralis* (Boulenger, 1900) (Squamata: Pareatidae), the description of a new species from Peninsular Malaysia, and the resurrection of *A. tropidonotus* (Lidth de Jue, 1923) from Sumatra: An integrative taxonomic analysis. Zootaxa 3664: 505–524. 10.11646. https://doi.org/10.11646/zootaxa.3664.4.5

Malkmus R, Manthey U, Vogel G, Hoffmann P, Kosuch J (2002) Amphibians and Reptiles of Mount Kinabalu (North Borneo). A.R.G. Ganter Verlag Kommanditgesellschaft, Ruggel, 424 pp.

Oskyrko O, Mi C, Meiri S, Du W (2024) ReptTraits: A comprehensive dataset of ecological traits in reptiles. Scientific Data 11: 243. https://doi.org/10.1038/s41597-024-03079-5

Ota H, Lin JT, Hirata T, Chen SL (1997) Systematic review of Colubrid snakes of the genus Pareas in the East Asian islands. Journal of Herpetology 31(1): 79–87. https://doi.org/10.2307/1565332

Pan T, Zhou WL, Shi WB, Zhao K, Chen JY, Wang WG, Chu J, Pu FG, Gu CM, Zhamg BW (2014) Species Richness of Amphibians and Reptiles in Dabie Mountains,China. Dongwuxue Zazhi 49(2): 195–206.

Posada D (2008) jModelTest: Phylogenetic model averaging. Molecular Biology and Evolution 25(7): 1253–1256. https://doi.org/10.1093/molbev/msn083

Poyarkov NA, Nguyen TV, Pawangkhanant P, Yushchenko PV, Brakels P, Nguyen LH, Nguyen HN, Suwannapoom C, Orlov N, Vogel G (2022) An integrative taxonomic revision of slug-eating snakes (Squamata, Pareidae, Pareineae) reveals unprecedented diversity in Indochina. PeerJ 10: e12713. https://doi.org/10.7717/peerj.12713

Rambaut A, Suchard M, Drummond AJ (2024) Tracer 1.6. http://tree.bio.ed.ac.uk/software/tracer/ [accessed on 11 March 2025].

Ronquist F, Teslenko M, van der Mark P, Ayres DL, Darlin A, Höhna S, Larget B, Liu L, Suchard MA, Huelsenbeck JP (2012) MrBayes 3.2: Efficient Bayesian phylogenetic inference and model choice across a large model space. Systematic Biology 61(3): 539–542. https://doi.org/10.1093/sysbio/sys029

Sambrook J, Fritsch EF, Maniatis T (1989) Molecular Cloning: A Laboratory Manual. 2nd edn. Cold Spring Harbor Laboratory Press, Cold Spring Habor, NY.

Silvestro D, Michalak I (2012) raxmlGUI: A graphical front-end for RAxML. Organisms, Diversity & Evolution 12: 335–337. https://doi.org/10.1007/s13127-011-0056-0

Stuebing RB, Inger RF, Lardner B (2014) A field guide to the snakes of Borneo. Natural History Publication, Borneo, Kota Kinabalu, 310 pp.

Suntrarachun S, Chanhome L, Hauser S, Sumontha M, Kanya K (2020) Molecular phylogenetic support to the resurrection of *Pareas macularius* from the synonymy of *Pareas margaritophorus* (Squamata: Pareidae). Tropical Natural History 20(2): 182–190. https://li01.tci-thaijo.org/index.php/tnh/article/view/176120

Uetz P, Freed P, Aguilar R, Reyes F, Kudera J Hošek J [Eds] (2025) The Reptile Database. http://www.reptile-database.org [accessed on 11 March, 2025]

Vogel G (2015) A new montane species of the genus *Pareas* Wagler, 1830 (Squamata: Pareatidae) from northern Myanmar. Taprobanica 7: 1–7. https://doi.org/10.47605/tapro.v7i1.148

Vogel G, Nguyen TV, Lalremsanga HT, Biakzuala L, Hrima V, Poyarkov NA (2020) Taxonomic Reassessment of the *Pareas margaritophorus-macularius* Species Complex (Squamata, Pareidae). Vertebrate Zoology 2020(70): 547–569. https://doi.org/10.4038/tapro.v7i1.7501

Vogel G, Nguyen TV, Zaw T, Poyarkov NA (2021) A new species of the *Pareas monticola* complex (Squamata, Serpentes, Pareidae) from Chin Mountains with additions to the Pareas fauna of Myanmar. Journal of Natural History 54: 2577–2612. https://doi.org/10.1080/00222933.2020.1856953

Wallach V, Williams KL, Boundy J (2014) Snakes of the World. A Catalogue of Living and Extinct Species; CRC Press: Boca Raton, FL, USA. https://doi.org/10.1201/b16901

Wang H, Luo X, Meng SQ, Bei YJ, Song T, Meng T, Li GF, Zhang BW (2015) The phylogeography and population demography of the Yunnan caecilian (*Ichthyophis bannanicus*): Massive rivers as barriers to gene flow. PLoS ONE 10(4): e0125770. https://doi.org/10.1371/journal.pone.0125770

Wang P, Che J, Liu Q, Li K, Jin JQ, Jiang K, Shi L, Guo P (2020) A revised taxonomy of Asia snail-eating snakes *Pareas* (Squamata, Pareidae): Evidence from morphological comparison and molecular phylogeny. ZooKeys 939: 45–64. https://doi.org/10.3897/zookeys.939.49309

Wu YH, Hou SB, Yuan ZY, Jiang K, Huang RY, Wang K, Liu Q, Yu ZB, Zhao HP, Zhang BL, Chen JM, Wang LJ, Stuart BL, Chambers EA, Wang YF, Gao W, Zou DH, Yan F, Zhao GG, Fu ZX, Wang SN, Jiang M, Zhang L, Ren JL, Wu YY, Zhang LY, Yang DC, Jin JQ, Yin TT, Li JT, Zhao WG, Murphy RW, Huang S, Guo P, Zhang YP, Che J (2023) DNA barcoding of Chinese snakes reveals hidden diversity and conservation needs. Molecular Ecology Resources 23(5): 1124–1141. https://doi.org/10.1111/1755-0998.13784

You CW, Poyarkov NA, Lin SM (2015) Diversity of the snail-eating snakes *Pareas* (Serpentes, Pareatidae) from Taiwan. Zoologica Scripta 44(4): 349–361. https://doi.org/10.1111/zsc.12111

Zhang CW, Liu K, Huang RY, Hu TL, Yu L, Sun RL, Zhang YC, Wen J, Zhang BW (2023) A New Species of the Genus *Achalinus* (Squamata, Xenodermidae) from the Dabie Mountains, Anhui, China. Animals 13(4): 708. https://doi.org/10.3390/ani13040708

Zhao EM (2006) Snakes of China. Anhui Science Technology Publishing House, Hefei, China. [in Chinese]

Zhao EM, Huang MH, Zong Y, Jiang YM, Huang QY, Zhao H, Ma JF, Zheng J, Huang ZJ, Wei G (1998) Fauna Sinica, Reptilia, Squamata. Serpentes. Science Press, Beijing, China. [in Chinese]

Supplementary material 1

Supplementary information

Authors: Cai-wen Zhang, Shi-hang Xu, Tao Luo, Chong Liu, Lei Yu, Jiang Zhou, Tao Pan, Bao-wei Zhang

Data type: docx

Explanation note: Text.

Copyright notice: This dataset is made available under the Open Database License (http://opendatacommons.org/licenses/odbl/1.0/). The Open Database License (ODbL) is a license agreement intended to allow users to freely share, modify, and use this Dataset while maintaining this same freedom for others, provided that the original source and author(s) are credited.

Link: https://doi.org/10.3897/zse.101.156697.suppl1